nature microbiology

Article

https://doi.org/10.1038/s41564-025-02140-2

Mycobacterium tuberculosis-derived linoleic acid increases regulatory T cell function to promote bacterial survival within macrophages

Received: 17 August 2024

Accepted: 2 September 2025

Published online: 10 October 2025

Check for updates

Hongyu Cheng[1,2,8], Shenzhi Li[1,2,8], Hongjie Liu[1,8], Meiyi Yan[3,8], Jingxiang Wang[2,8], Jingping Huang[2], Shanshan Liu[2], Yifan Yang[2], Xinyu Cao[2], Pengfei Cui[2], Yuanna Cheng[2], Zhonghua Liu[1], Jie Wang[1], Xiaochen Huang[1], Lin Wang[1], Lianhua Qin[1], Ruijuan Zheng[1], Carl G. Feng[4,5], Qiang Zou[6], Yicheng Sun[3] ✉, Zhe Ji[1,2] ✉, Hua Yang[1,2] ✉ & Baoxue Ge[1,2,7] ✉

Regulatory T (T_{reg}) cells expand during *Mycobacterium tuberculosis* (Mtb) infection and suppress T cell-mediated control. Whether Mtb actively contributes to this process is unclear. Here, using a genome-wide mutant library, we show that the expression of Mtb Rv1272c, an ATP-binding cassette transporter, increased under hypoxic conditions and promotes Mtb survival in vivo by increasing lecithin import, followed by the production and release of linoleic acid. Linoleic acid released by infected macrophages promoted surface trafficking of the immune checkpoint molecule cytotoxic T lymphocyte antigen 4 (CTLA-4) in T_{reg} cells via the Ca^{2+} transporter ATP2a3. This in turn inhibited macrophage reactive oxygen species production and promoted Mtb survival inside macrophages. Rv1272c-induced linoleic acid further promoted Mtb immune evasion by increasing CTLA-4 surface trafficking on T_{reg} cells in vivo. Mechanistically, linoleic acid interacts with ATP2a3 in T_{reg} cells and promotes mitochondria-associated endoplasmic reticulum (ER) membrane formation. This facilitates ER-to-mitochondria Ca^{2+} transfer and depletion of Ca^{2+} in the ER, and triggers store-operated calcium entry, thus elevating cytosolic Ca^{2+} levels to increase Ca^{2+}-dependent CTLA-4 surface trafficking in T_{reg} cells. These findings reveal that Mtb can use a metabolite to manipulate host responses and promote its intracellular survival.

Mycobacterium tuberculosis (Mtb) uses many intricate strategies to resist or impair the myriads of macrophage defences to enhance its intracellular survival, enabling its persistence and proliferation within the lungs[1]. As shown recently, D-serine, a metabolite produced by Mtb under hypoxic conditions, selectively inhibits interferon-γ (IFNγ) production by T cells, particularly $CD8^+$ T cells, thus eliminating the enhancement of T cells on antimicrobial capacities of macrophages[2]. However, whether and how Mtb manipulates other adaptive immune cells to promote its infection remains to be elucidated.

Although regulatory T (T_{reg}) cells hinder Mtb eradication by suppressing $CD4^+$ T cell responses[3], the immunosuppressive cytokines interleukin-10 (IL-10) and transforming growth factor-β (TGFβ) produced by T_{reg} cells appear to have a less important role in this context. Instead, T_{reg} cells impede effective anti-mycobacterial immunity primarily by inhibiting the production of key cytokines, such as IFNγ

A full list of affiliations appears at the end of the paper. ✉e-mail: sunyc@ipbcams.ac.cnyang; jizhe@tongji.edu.cn; yanghua97065@tongji.edu.cn; gebaoxue@sibs.ac.cn

and interleukin-17 (IL-17), which are essential for controlling Mtb infection[4]. T_{reg} cells are expanded in patients infected with Mtb and suppress antigen-specific production of IFNγ by effector T cells[5]. Similarly, in Mtb-infected mice, T_{reg} cells expand and restrict bacterial clearance in the lungs[3]. Furthermore, the T_{reg} cells arising in these infected mice delay the recruitment of effector T cells into the infected lungs, prolonging the initial phase of bacterial expansion[6]. However, it remains unclear whether and how Mtb explores T_{reg} cells to regulate antimicrobial capacities of macrophages.

As a key immune checkpoint molecule, cytotoxic T lymphocyte antigen 4 (CTLA-4) is highly constitutively expressed on T_{reg} cells and mediates critical immunosuppressive functions including the downregulation of ligand expression and transmission of inhibitory signals[7]. It has been shown that genetic polymorphisms of the *CTLA4* gene are associated with tuberculosis (TB) susceptibility[8]. Patients with latent TB have higher levels of CTLA-4 in lymphocytes compared with healthy controls[9]. Cell-surface CTLA-4 expression was higher on Mtb-specific T_{reg} cells than on Foxp3-conventional $CD4^+$ T cells in pulmonary lymph nodes of Mtb-infected mice[10]. However, the function of CTLA-4 in mediating immune responses to Mtb infection remains unclear.

Here we found that Mtb Rv1272c, an ATP-binding cassette (ABC) transporter, enhanced the import of lecithin and generation of linoleic acid. Rv1272c-induced linoleic acid facilitated cytosolic calcium ion (Ca^{2+})-mediated CTLA-4 trafficking to T_{reg} surfaces through the sarco/endoplasmic reticulum (SR/ER) Ca^{2+} ATPase pump (ATP2a3, also known as SERCA3), which restrained reactive oxygen species (ROS) production in macrophages, thereby boosting intracellular Mtb survival.

Results

Rv1272c promotes Mtb survival by inducing linoleic acid

To identify Mtb genes required for its in vivo survival, the genome-wide knockout (KO) mutant library of Mtb[11] was screened to identify Mtb mutants that failed to survive during lung infections in C57BL/6 mice (Extended Data Fig. 1a,b). The most significant Mtb in vivo survival essential gene Rv3682 has already been shown to be essential for the survival of Mtb at a low pH or in mice[12]. We then focused on the second highly significant in vivo survival essential gene Rv1272c (Fig. 1a, Supplementary Table 1 and Extended Data Fig. 1c), a member of ABC transporter type exporters[13]. The lung tissues of the Mtb H37Rv-infected C57BL/6 mice showed a hypoxic state[2]. We found that the production of Rv1272c in the Mtb H37Rv strain was significantly increased under hypoxic conditions (Extended Data Fig. 1d). To examine the contribution of Rv1272c to Mtb infection in vivo, we generated the Rv1272c KO strain H37RvΔRv1272c and Rv1272c complemented strain H37Rv(ΔRv1272c + Rv1272c) (Extended Data Fig. 1e). C57BL/6 mice infected with H37RvΔRv1272c (Fig. 1b and Extended Data Fig. 1f) had much lower bacterial burdens (Fig. 1c,d) and a milder lung pathology (Fig. 1e,f) than mice infected with the Mtb H37Rv strain, or Rv1272c complemented strain at 4 weeks post infection (wpi).

Rv1272c is predicted as a member of ABC transporter type exporters of Mtb long-chain fatty acids (FAs)[14]. Our comparative metabolomics analyses of the culture supernatants of bone marrow-derived macrophages (BMDMs) infected with H37Rv or H37RvΔ1272c by using gas chromatography–mass spectrometry (GC–MS) revealed that deletion of Rv1272c significantly downregulated linoleic acid levels (Fig. 1g, Extended Data Fig. 1g and Supplementary Table 2), which was independently validated through targeted linoleic acid quantification via GC–MS, revealing coordinated linoleic acid reduction in both cell lysates and culture supernatants of H37RvΔ1272c-infected BMDMs (Extended Data Fig. 1h,i). Consistently, mice infected with either H37Rv or the complemented strain, rather than H37RvΔRv1272c mutant at 4 wpi, showed elevated linoleic acid levels in lung homogenate supernatants (Fig. 1h), but not in serum (Fig. 1i). Moreover, deletion of Rv1272c reduced the linoleic acid level in both the lysates and culture supernatants from the H37Rv strain cultured in vitro (Extended Data Fig. 1j,k).

Linoleic acid is generated from lecithin, which is processed by phospholipaseA2 (PLA2)[15]. We found that exogenous lecithin supplementation significantly increased the levels of lecithin within the H37Rv or H37Rv(ΔRv1272c + Rv1272c) strain, but not within the H37RvΔRv1272c strain (Extended Data Fig. 1l) cultured in vitro. Conversely, extracellular lecithin levels showed an inverse dynamic: culture supernatants of the H37Rv or H37Rv(ΔRv1272c + Rv1272c) strain showed substantial depletion, while supernatants from the H37RvΔRv1272c strain showed minimal reduction (Extended Data Fig. 1m). Meanwhile, the levels of linoleic acid were significantly enhanced by supplementation of lecithin in the H37Rv or H37Rv(ΔRv1272c + Rv1272c) strain, but not within the H37RvΔRv1272c strain (Fig. 1j,k). Consistently, lecithin supplementation also markedly increased the levels of linoleic acid exclusively in H37Rv- or H37Rv(ΔRv1272c + Rv1272c)-infected BMDMs, but not in H37RvΔRv1272c-infected BMDMs (Figs. 1l,m and Extended Data Fig. 1n).

Fatty acid efflux regulators in macrophages include fatty acid-binding and transport proteins (FABPs and FATPs)[16], lipocalin-family member Obp2a (ref. 17) and ABC transporters (ABCA1 and ABCG1)[18]. In Mtb H37Rv-infected BMDMs, *Abcg1* knockdown significantly reduced extracellular linoleic acid levels and abrogated Rv1272c-mediated enhancement of linoleic acid secretion, whereas knockdown of *Fabp4*, *Fabp5*, *Fatp1*, *Fatp2*, *Abca1* or *Obp2a* had no significant effect (Extended Data Fig. 2a–i). Meanwhile, deletion of Rv1272c did not significantly change the level of *Fabp4*, *Fabp5*, *Fatp1* and *Fatp2* mRNA in BMDMs infected with H37Rv (Extended Data Fig. 2j–m).

Using GC–MS, we observed that administration of linoleic acid significantly increased linoleic acid levels in the lung tissues or serum of mice infected with H37Rv and H37RvΔRv1272c strains compared with the control (Extended Data Fig. 2n–p). Moreover, linoleic acid treatment rescued the impaired in vivo survival and histopathological damage linked to the Rv1272c deletion in the lung tissues of the infected mice at 4 wpi (Fig. 1n–p).

Fig. 1 | Rv1272c promotes mycobacterial survival in vivo via linoleic acid. **a**, Volcano plot of Mtb survival essential genes screened at 4 wpi in mice. The blue dots indicate genes essential for Mtb in vivo survival at this timepoint. **b**–**f**, C57BL/6 mice were aerosol infected with ~200 colony-forming units (c.f.u.) per mouse of indicated Mtb strains. A schematic representation of the mouse experimental design is shown in **b**; after 4 weeks of infection, histopathological analysis of lung sections from infected mice was performed using acid-fast staining (**c**; scale bars, 100 μm (upper) and 20 μm (lower)), bacterial c.f.u. (**d**), H&E staining (scale bar, 1 mm; with values for quantified inflammatory area of each section) (**e**) and quantified inflammatory areas (**f**). **g**, Heatmap showing parts of the metabolites differentially in culture supernatants of Mtb-infected BMDMs for 24 h (NI, not infected. Red: upregulation. Blue: downregulation). **h**,**i**, C57BL/6 mice were aerosol infected with ~200 c.f.u. per mouse of indicated Mtb strains. Linoleic acid (LA) concentrations in lung homogenate supernatants (**h**) and serum (**i**) were analysed at 4 wpi. **j**,**k**, Assay of linoleic acid concentration from lysis (**j**) or culture supernatants (**k**) of Mtb treated with or without lecithin (100 μM) for 14 days. **l**,**m**, After Mtb strains were incubated with or without lecithin (100 μM) for 14 days, the concentration of linoleic acid in the cell lysis (**l**) and culture supernatants (**m**) of Mtb-infected BMDMs for 24 h was assayed. **n**–**p**, C57BL/6 mice were aerosol infected with ~200 c.f.u. per mouse of indicated Mtb strains and treated with or without linoleic acid. After 4 weeks of infection, histopathological analysis of lung sections from infected mice was performed using H&E staining (scale bar, 1 mm; with values for quantified inflammatory area of each section) (**n**) and quantified inflammatory areas (**o**), and bacterial c.f.u. (**p**) were quantified. Data in **a** and **c**–**p** represent one experiment with three independent biological replicates ($n = 3$); mean ± s.e.m. A two-sided negative binomial test with the MAGeCK algorithm (**a**), two-tailed unpaired Student's *t*-tests (**d**,**f**,**h**,**i**,**o**,**p**) and two-way ANOVA with Tukey's multiple-comparison test (**j**–**m**) were used for statistical analyses.

https://doi.org/10.1038/s41564-025-02140-2

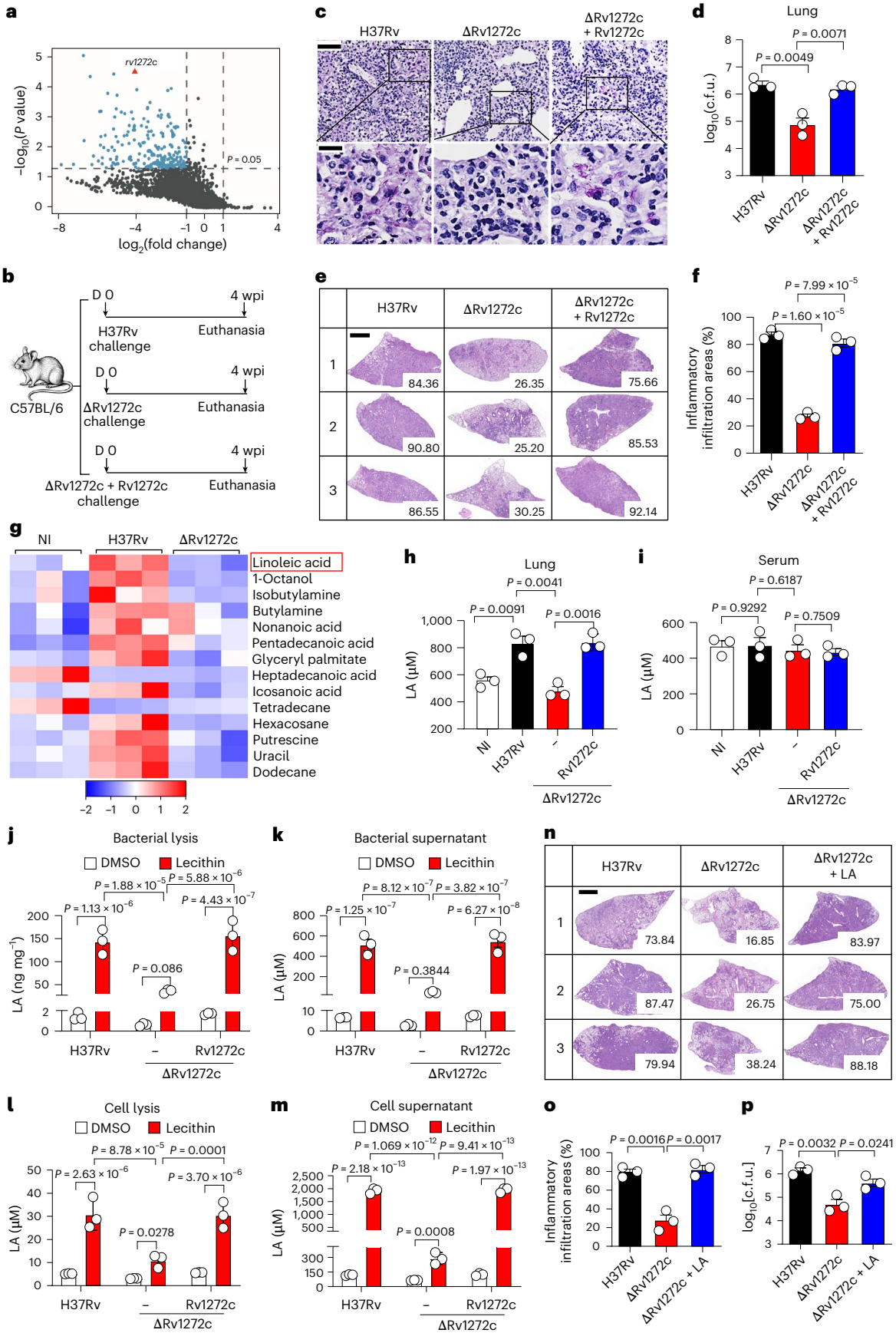

Linoleic acid promotes T_{reg} cell-mediated Mtb immune evasion

We found that deletion of Rv1272c (Fig. 2a) or treatment of linoleic acid (Fig. 2b) did not significantly alter Mtb growth in vitro. Given the well-established role of phthiocerol dimycocerosate (PDIM) in Mtb virulence[19], an analysis of PDIM[20] revealed comparable levels in WT H37Rv, H37RvΔRv1272c mutant and complemented strains under standardized in vitro culture conditions (Extended Data Fig. 3).

Deletion of Rv1272c (Fig. 2c) or treatment of linoleic acid (Fig. 2d) did not significantly change the intracellular survival of Mtb H37Rv in BMDMs, and had no significant impact on the bacterial load or pathology damage in the lung tissues of Mtb-infected *Rag1*$^{-/-}$ mice (Extended Data Fig. 4a–d). In addition, we observed no significant differences in CD45^{+}Ly6G^{+} neutrophil[21] percentages within lung tissues between WT- and H37RvΔRv1272c-infected mice (Extended Data Fig. 5a).

Deletion of Rv1272c did not significantly change the percentages of CD4^{+}T-bet^{+} T (Th1) (Fig. 2e), CD8^{+}T-bet^{+} T (Tc1) (Fig. 2f) or CD4^{+}Foxp3^{+} (T_{reg}) cells (Fig. 2g) in lung tissues from Mtb-infected mice[22]. In addition, the absence of Rv1272c did not notably impact the IFNγ concentration in serum or lung tissues of Mtb-infected mice (Extended Data Fig. 5b,c), and did not significantly change the anti-inflammatory cytokine production or release, as indicated by levels of TGFβ (Extended Data Fig. 5d,e) and IL-10 (Extended Data Fig. 5f,g) in serum or lung tissues of Mtb-infected mice. However, deletion of Rv1272c significantly reduced the level of membrane CTLA-4 on T_{reg} cells from the lung tissues of H37Rv-infected mice (Fig. 2h), while total CTLA-4 protein levels did not show significant changes (Fig. 2i). Furthermore, linoleic acid enhanced CTLA-4 surface trafficking on lung-derived T_{reg} cells from H37Rv-infected mice (Extended Data Fig. 5h) and rescued the impaired membrane localization of CTLA-4 caused by Rv1272c deletion (Fig. 2h).

Depletion of T_{reg} cells eliminated the increased effect of Rv1272c or linoleic acid on the in vivo survival of Mtb in diphtheria toxin (DT)-injected *Foxp3*^{DTR} mice[23] (Extended Data Fig. 5i and Fig. 2j,k). Also, deletion of Rv1272c significantly reduced the bacterial load in lung tissues of WT or *Rag1*$^{-/-}$ mice transferred with T_{reg} cells, which was eliminated by the addition of linoleic acid (Fig. 2l). Intriguingly, Rv1272c or linoleic acid promoted the intracellular survival of Mtb in BMDMs only in the presence of T_{reg} cells (Fig. 2m,n), but did not significantly change T_{reg} proportions in the co-culture model (Extended Data Fig. 5j–l).

Rv1272c and linoleic acid upregulate T_{reg} cell CTLA-4 trafficking

BMDMs infected with the Rv1272c KO strain or supplied with linoleic acid did not significantly change the level of TGFβ (Fig. 3a,b) and IL-10 (Fig. 3c,d) in supernatants when co-cultured with T_{reg} cells. Also, the deletion of Rv1272c did not significantly change the total level of CTLA-4 in T_{reg} cells (Fig. 3e); however, BMDMs infected with the Rv1272c KO strain markedly lowered CTLA-4 surface trafficking on T_{reg} cells (Fig. 3f), but treatment of linoleic acid eliminated the decrease (Extended Data Fig. 5m), which was also observed in the lung tissues (Fig. 2h,i) or spleens of H37Rv-infected mice (Extended Data Fig. 5n,o). CTLA-4 is constitutively expressed on the surface of T_{reg} cells to drive their suppressive functions[7]. The addition of linoleic acid did not significantly change the T_{reg} cell differentiation in vitro (Extended Data Fig. 6a), or the total level of CTLA-4 (Extended Data Fig. 6b), but markedly promoted the surface trafficking of CTLA-4 on T_{reg} cells (Extended Data Fig. 6c,d).

Administration of anti-CTLA-4 blocking antibody markedly reduced the bacterial loads (Fig. 3g) and pathology (Extended Data Fig. 6e,f) in the lung tissues of Mtb H37Rv-infected mice, suggesting an unexpected therapeutic effect of anti-CTLA-4 on TB. Consistently, promotional effects of Rv1272c or linoleic acid on Mtb survival were not observed in mice injected with the anti-CTLA-4 antibody (Fig. 3g). To exclude potential confounders linked to T_{reg} depletion[24], we performed additional flow cytometry (FCM) analysis of lung T_{reg} cell populations. Treatment of Mtb H37Rv-infected mice with anti-CTLA-4 blocking antibody did significantly change T_{reg} cell percentages compared with those counterparts treated with isotype-matched IgG antibody controls (Extended Data Fig. 6g). Besides, we intercrossed *Ctla4*-floxed mice with *Foxp3*^{CreERT2} transgenic mice to produce *Ctla4*$^{fl/+}$*Foxp3*^{CreERT2} mice, which were subsequently infected with H37Rv, H37RvΔRv1272c strains supplemented with or without linoleic acid, using *Ctla4*$^{fl/+}$ mice as control. Conditional knockdown of CTLA-4 in Foxp3-expressing cells attenuated the promotional effects of Rv1272c or linoleic acid on the bacterial loads in the lung tissues of H37Rv-infected mice (Fig. 3h). Consistently, the attenuated survival of the H37RvΔRv1272c strain in BMDMs compared with that of Mtb H37Rv was abrogated by CTLA-4 blockade in T_{reg} cells (Fig. 3i).

CTLA-4 inhibits ROS production in macrophages

WT H37Rv- or H37RvΔRv1272-infected BMDMs were pretreated with N-acetyl-L-cysteine (NAC; inhibitor of ROS)[25], 3-methyladenine (3-MA; inhibitor of autophagy)[26], benzyloxycarbonyl-Val-Ala-Asp-fluoromethyl ketone (Z-VAD; inhibitor of apoptosis)[27], aminoguanidine hydrochloride (AGHS; inhibitor of nitric oxide synthase)[28] or bafilomycin A1 (BafA1; inhibitor of lysosome acidification)[29] and then co-cultured with T_{reg} cells treated with isotype control IgG or anti-CTLA-4 blocking antibody. Only NAC treatment abolished the difference of Mtb survival in BMDMs co-cultured with T_{reg} cells (Fig. 4a and Extended Data Fig. 7a). It has been reported that CTLA-4 inhibits ROS production in tumour[30] and T cells[31]. We found that H37RvΔRv1272-infected mice had significantly elevated cytosol ROS levels in macrophages from lung tissues of the Mtb-infected mice (Fig. 4b,c). Furthermore, *Foxp3*^{DTR} mice injected with DT (Fig. 4b) or WT mice injected with anti-CTLA-4 blocking antibody (Fig. 4c) eliminated the suppressive effects of Rv1272c on ROS production. Consistently, when co-cultured with T_{reg} cells, BMDMs infected with the H37RvΔRv1272 strain showed significantly higher cytosol ROS levels than those cells infected with the H37Rv strain, which was eliminated by treatment of linoleic acid (Fig. 4d). Moreover, blockade of CTLA-4 on T_{reg} cells in the co-culture model eliminated the inhibitory

Fig. 2 | Rv1272c and linoleic acid promote mycobacterial survival via T_{reg} cells. **a**,**b**, In vitro growth curves of indicated Mtb strains (**a**) or H37Rv ± linoleic acid (**b**) over 14 days (37 °C). **c**, Intracellular c.f.u. in BMDMs infected with the H37Rv or ΔRv1272c strain. **d**, BMDMs were infected with H37Rv and treated with linoleic acid or DMSO. Intracellular c.f.u. were determined for indicated times. **e**–**g**, C57BL/6 mice were aerosol infected with indicated Mtb strains (~200 c.f.u.) for 4 weeks. Percentages of CD4^{+}T-bet^{+} (**e**), CD8^{+}T-bet^{+} (**f**) and CD4^{+}Foxp3^{+} T cells (**g**) were measured using flow cytometry (FCM). **h**,**i**, C57BL/6 mice were aerosol infected with indicated Mtb strains (~200 c.f.u.) and treated with or without linoleic acid for 4 weeks. Mean fluorescence intensity (MFI) of membrane CTLA-4 levels (**h**) and total CTLA-4 levels (**i**) were measured in CD4^{+} T_{reg} cells by FCM. **j**, C57BL/6 or *Foxp3*^{DTR} mice treated with diphtheria toxoid (DT) or PBS at indicated times were aerosol infected with indicated Mtb strains (~200 c.f.u.). Bacterial burdens in mouse lungs were assayed by c.f.u. at 4 wpi. **k**, C57BL/6 or *Foxp3*^{DTR} mice treated with DT or PBS at indicated times were aerosol infected with indicated Mtb strains (~200 c.f.u.) and treated with or without linoleic acid. The bacterial burdens in the lungs were assayed by c.f.u. at 4 wpi. **l**, WT, *Rag1*$^{-/-}$ and *Rag1*$^{-/-}$ mice adoptively transferred with T_{reg} cells (*Rag1*$^{-/-}$ + T_{reg}) were aerosol infected with indicated Mtb strains (~200 c.f.u.) and treated with or without linoleic acid. The bacterial load in lungs at 4 wpi was assayed by c.f.u. **m**, After 1 day of infection with Mtb strains, BMDMs were co-incubated with or without CD4^{+} T_{reg} cells for 1 day, and intramacrophage survival of Mtb was assayed by c.f.u. **n**, After 1 day of infection with indicated Mtb strains, BMDMs were co-incubated with or without CD4^{+} T_{reg} cells treated with or without linoleic acid for 1 day, and the intracellular c.f.u. of Mtb were determined. Data in **a**–**n** represent one experiment with three independent biological replicates ($n = 3$); mean ± s.e.m. Two-way ANOVA with Tukey's multiple-comparison test (**a**–**d**,**j**–**n**) and two-tailed unpaired Student's *t*-tests (**e**–**i**) were used for statistical analyses.

https://doi.org/10.1038/s41564-025-02140-2

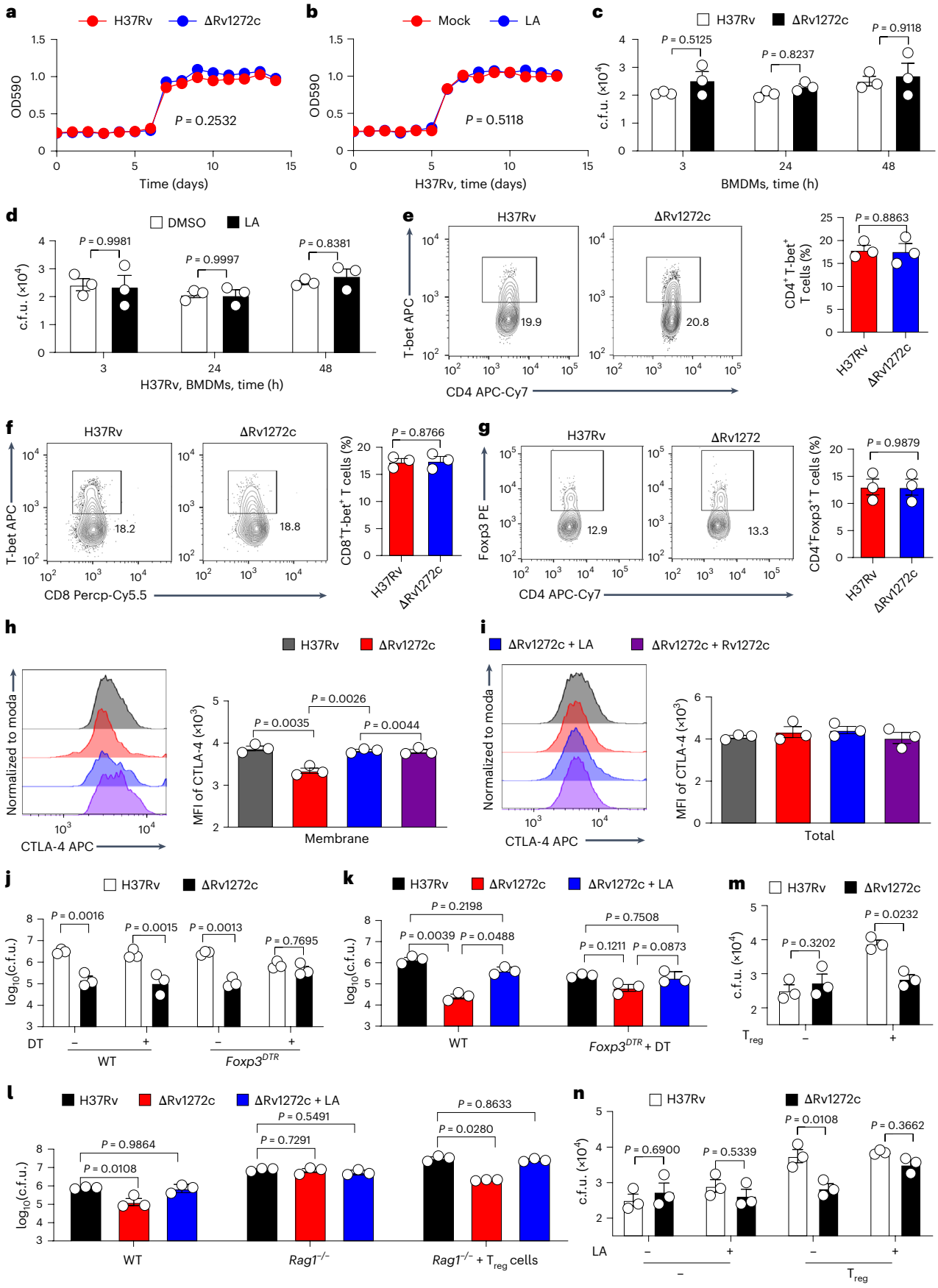

https://doi.org/10.1038/s41564-025-02140-2

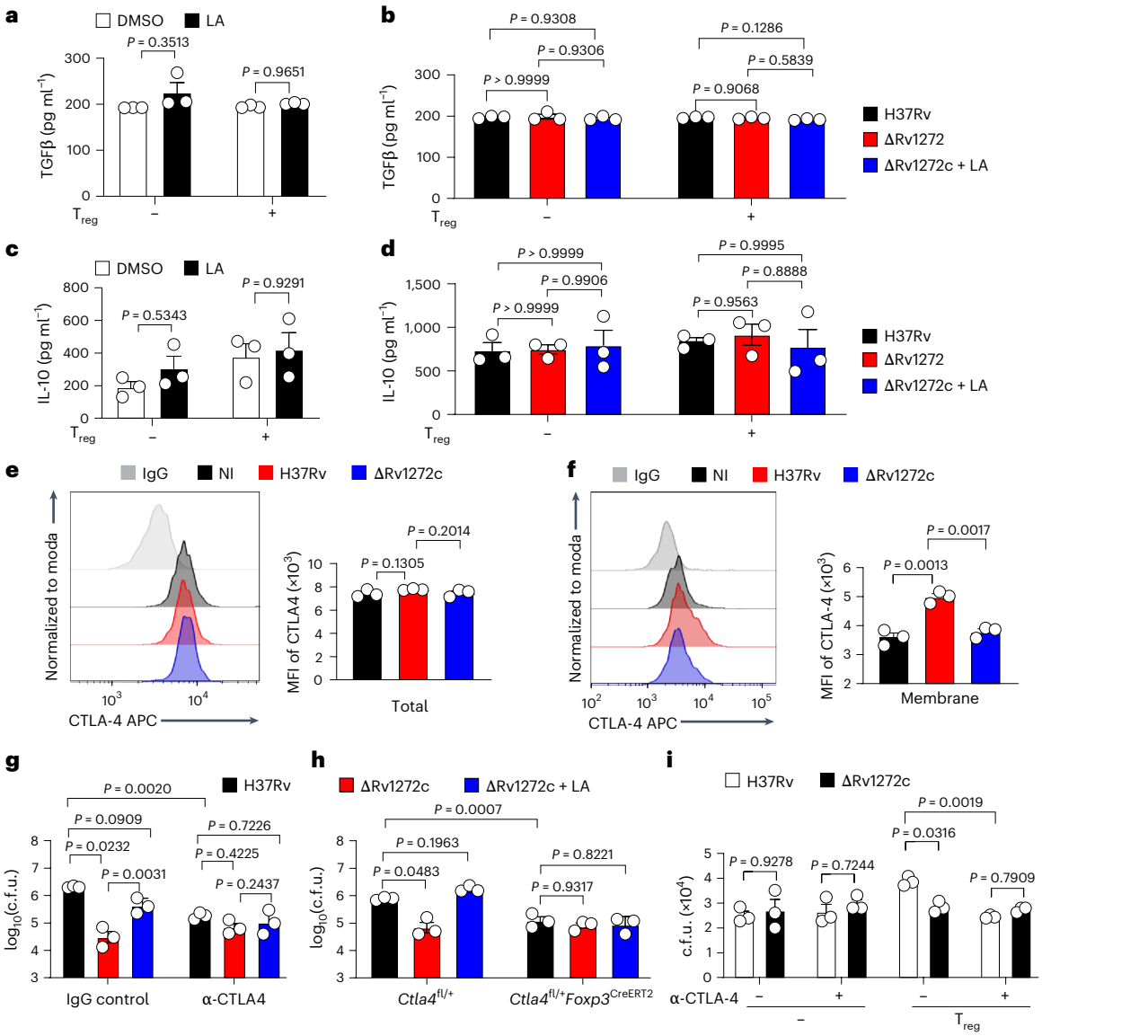

Fig. 3 | Rv1272c and linoleic acid enhance CTLA-4 surface trafficking on T_{reg} cells. a–**d**, After 1 day of infection with H37Rv (**a**,**c**) or indicated Mtb strains (**b**,**d**), BMDMs were co-incubated with or without $CD4^+$ T_{reg} cells treated with or without linoleic acid for 1 day; TGFβ (**a**,**b**) and IL-10 (**c**,**d**) levels in the culture supernatant were measured by ELISA. **e**,**f**, After 1 day of infection with indicated Mtb strains, BMDMs were co-incubated with $CD4^+$ T_{reg} cells for 1 day and the MFIs of total CTLA-4 levels (**e**) and membrane CTLA-4 levels (**f**) in $CD4^+$ T_{reg} cells were measured by FCM. **g**, C57BL/6 mice treated with isotype control IgG or anti-CTLA-4 antibodies (500 μg per mouse) on 4, 8, 12, 16, 20 and 24 days post infection were aerosol infected with approximately 200 c.f.u. per mouse of indicated Mtb strains; then, the infected mice were treated with or without linoleic acid via drinking water. After 4 weeks of infection, bacterial burdens in mouse lungs were measured using c.f.u. assay. **h**, *Ctla4*$^{fl/+}$ or *Ctla4*$^{fl/+}$*Foxp3*^{CreERT2} mice treated with tamoxifen at 4, 8, 12, 16, 20 and 24 days post infection were aerosol infected with approximately 200 c.f.u. per mouse of indicated Mtb strains for 4 weeks. Bacterial burdens in mouse lungs were measured using c.f.u. assay. **i**, After 1 day of infection with indicated Mtb strains, BMDMs were co-incubated with or without $CD4^+$ T_{reg} cells treated with isotype control IgG or anti-CLTA-4 antibodies (40 μg ml^{-1}) for 1 day. The bacterial burdens in BMDMs were measured at 2 days after infection. Data in **a**–**i** represent one experiment with three independent biological replicates ($n = 3$); mean ± s.e.m. Two-way ANOVA with Tukey's multiple-comparison test (**a**–**d**,**g**–**i**) and two-tailed unpaired Student's *t*-tests (**e**,**f**) were used for statistical analyses.

effect of Rv1272c or linoleic acid on the cytosol ROS levels in macrophages (Fig. 4d).

Early secreted antigenic target 6 $(ESAT\text{-}6)_{4–17}$-specific T_{reg} cells were pooled and enriched from C7 TCR tg.CD90.1 mice[10,32]. After differentiation in vitro, $ESAT\text{-}6_{4–17}$-specific T_{reg} cells were then co-incubated with BMDMs infected with H37Rv or H37RvΔRv1272 strains and extra addition of linoleic acid. BMDMs infected with the H37RvΔRv1272 strain markedly lowered CTLA-4 surface trafficking on $ESAT\text{-}6_{4–17}$-specific T_{reg} cells, but treatment of linoleic acid retained the surface level of CTLA-4 (Extended Data Fig. 7b). Similarly, BMDMs co-cultured with $ESAT\text{-}6_{4–17}$-specific T_{reg} cells showed much higher cytosol ROS levels when infected with the H37RvΔRv1272 strain than the WT strain, which was eliminated by treatment of linoleic acid (Extended Data Fig. 7c).

Linoleic acid promotes Ca^{2+} levels in the cytosol of T_{reg} cells

CTLA-4 transportation to the cell surface is linked to Ca^{2+} flow[33]. A Ca^{2+}-specific chelator, ethylene glycol tetraacetic acid (EGTA), eliminated the promotional effects of linoleic acid on CTLA-4 surface trafficking (Fig. 5a). Indeed, treatment of linoleic acid promoted Ca^{2+} levels in the cytosol of T_{reg} cells ex vivo (Figs. 5b,c). Consistently, BMDMs infected with H37RvΔRv1272 significantly downregulated Ca^{2+} levels in the cytosol of co-cultured T_{reg} cells, which was eliminated by treatment of linoleic

https://doi.org/10.1038/s41564-025-02140-2

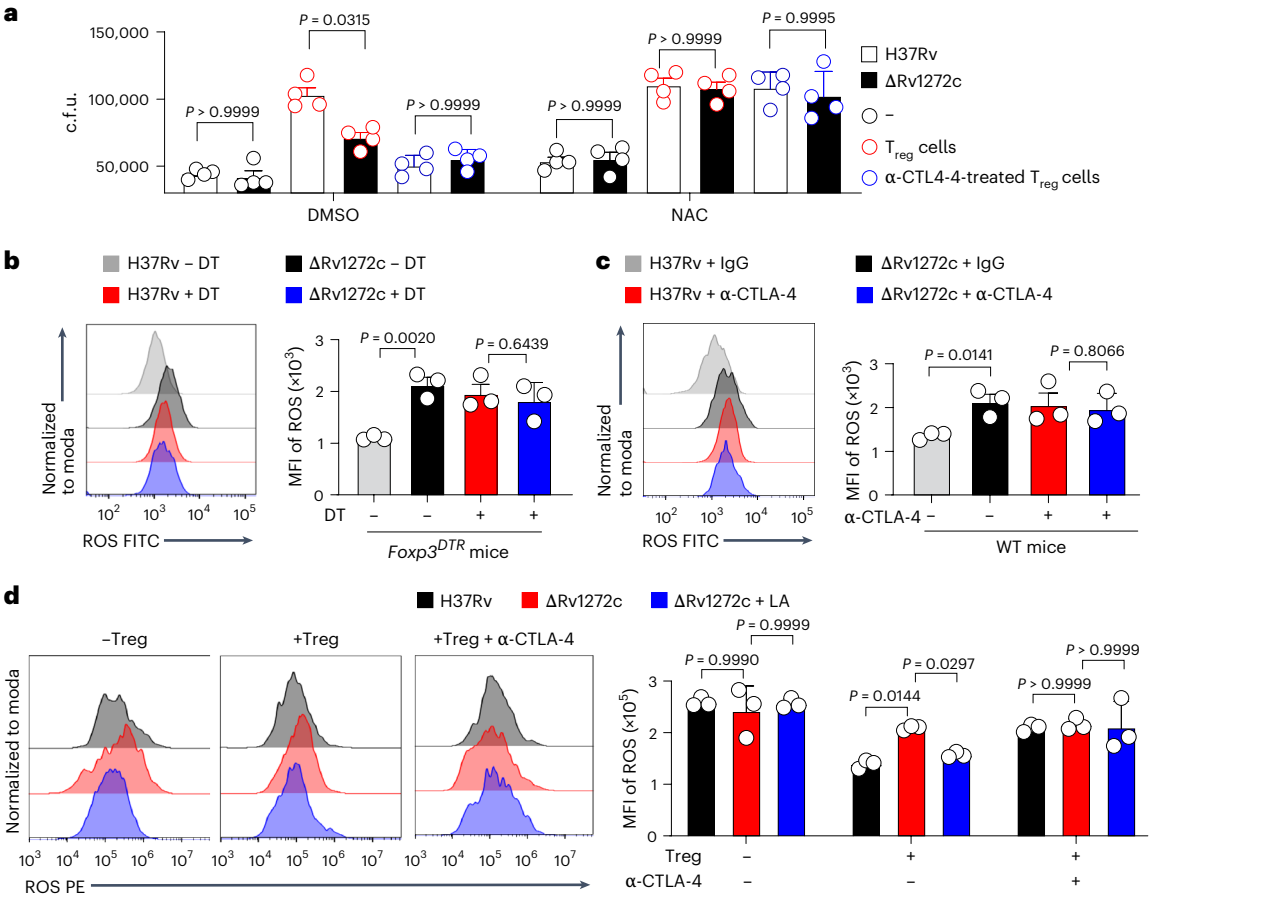

Fig. 4 | Rv1272c impairs the anti-mycobacterial ability of macrophages through CTLA-4-mediated inhibition of ROS. a, Mtb-infected BMDMs were pretreated with DMSO or NAC (ROS inhibitor) for 24 h and then co-cultured with T_{reg} cells treated with isotype control IgG or anti-CTLA-4 blocking antibody (40 μg ml^{-1}) for 1 day; intracellular survival of the indicated Mtb strains in BMDMs infected for 2 days was determined using a c.f.u. assay. **b**, C57BL/6 or *Foxp3*^{DTR} mice treated with DT or PBS at 4, 8, 12, 16, 20 and 24 days post infection were aerosol infected with approximately 200 c.f.u. per mouse of indicated Mtb strains for 4 weeks. The MFI of ROS levels in F4/80$^+$ macrophages sorted from lung tissues was measured by FCM. **c**, C57BL/6 mice treated with isotype control IgG or anti-CTLA-4 antibodies (500 μg per mouse) were aerosol infected with approximately 200 c.f.u. per mouse of indicated Mtb strains for 4 weeks. The MFI of ROS levels in F4/80$^+$ macrophages sorted from lung tissues was measured by FCM. **d**, After 1 day of infection with indicated Mtb strains, BMDMs were co-incubated with or without CD4$^+$ T_{reg} cells treated with or without linoleic acid, or with isotype control IgG or anti-CLTA-4 antibodies (40 μg ml^{-1}) for 1 day; the MFI of ROS levels in BMDMs was measured by FCM. Data in **a**–**d** represent one experiment with at least three independent biological replicates (**a**, $n = 4$; **b**–**d**, $n = 3$); mean ± s.e.m. Two-way ANOVA with Tukey's multiple-comparison test (**a**,**d**) and two-tailed unpaired Student's *t*-tests (**b**,**c**) were used for statistical analyses.

acid (Fig. 5d). In T cells, increased cytosolic Ca^{2+} levels predominantly originate from the release of ER stores, or extracellular influx through the plasma membrane (PM) channels[34]. Our immunofluorescence analysis showed that linoleic acid was mainly located in the ER of T_{reg} cells (Fig. 5e). Addition of linoleic acid (100 μM) reduced Ca^{2+} levels in the ER of T_{reg} cells (Figs. 5f,g), but deletion of Rv1272c elevated ER Ca^{2+} stores in T_{reg} cells co-cultured with Mtb H37Rv-infected BMDMs, which was completely reversed by exogenous linoleic acid supplementation (Fig. 5h). Reduced Ca^{2+} levels in the ER trigger store-operated calcium entry (SOCE), thereby potentiating extracellular Ca^{2+} influx into the cytosol and elevating cytosolic Ca^{2+} levels[35]. We found that treatment of linoleic acid induced the potentiation of SOCE in T_{reg} cells (Fig. 5i).

Mitochondria-associated ER membranes (MAMs) promote Ca^{2+} transfer from the ER to mitochondria[36]. Linoleic acid promoted the formation of MAMs[37] to facilitate ER Ca^{2+} transfer into mitochondria through the mitochondrial calcium uniporter (MCU)[34]. We found that linoleic acid treatment enhanced MAM formation in T_{reg} cells (Extended Data Fig. 8), but treatment of the MCU inhibitor, carbonyl cyanide 4-(trifluoromethoxy) phenylhydrazone (FCCP)[38], enabled linoleic acid to paradoxically enhance Ca^{2+} levels in the ER of T_{reg} cells (Figs. 5j,k). Consistently, deletion of Rv1272c significantly reduced ER Ca^{2+} stores in T_{reg} cells co-cultured with H37Rv-infected BMDMs under FCCP treatment, a perturbation completely reversed by exogenous linoleic acid supplementation (Fig. 5l).

Linoleic acid interacts with ATP2a3

By performing immunoprecipitation (IP) and MS analysis in splenic cells, we found that linoleic acid interacted with ATP2a3, a P-type Ca^{2+} transporter (Extended Data Fig. 9a)[39], which was further confirmed by co-IP studies in splenic cells (Fig. 6a), immunofluorescence analysis in T_{reg} cells, pull-down assay (Extended Data Fig. 9b,c) and surface plasmon resonance (SPR) assay (Fig. 6b). Linoleic acid was predicted to potentially interact with the ATPase catalytic pocket of ATP2a3 (Extended Data Fig. 9d). Indeed, the presence of linoleic acid enhanced ATP2a3 enzymatic activity[40] (Fig. 6c). Knockdown of *Atp2a3* by specific small interfering RNA (siRNA) in T_{reg} cells (Extended Data Fig. 9e) abolished linoleic acid-induced MAMs or SOCE in T_{reg} cells (Fig. 6d,e). Furthermore, *Atp2a3* knockdown abrogated Rv1272c- or linoleic acid-induced enhancement of CTLA-4 surface trafficking in T_{reg} cells, and the enhanced effect of Rv1272c or linoleic acid on the intracellular survival of Mtb H37Rv in BMDMs (Fig. 6f–h). Furthermore, *Atp2a3* knockdown (Extended Data Fig. 9f) eliminated the promotional effects of linoleic acid or Rv1272c on CTLA-4 surface trafficking in T_{reg} cells (Fig. 6i) and Mtb survival in vivo (Fig. 6j).

https://doi.org/10.1038/s41564-025-02140-2

Discussion

Adaptations to the host immune microenvironment are important for Mtb to establish chronic pathogenesis[1,41]. Our genome-wide clustered regularly interspaced short palindromic repeats (CRISPR) KO screening identifies Rv1272c as an essential gene for Mtb in vivo survival, which is consistent with a previous finding that Rv1272c is also required for Mtb growth in the C57BL/6J mouse spleen, by transposon site hybridization (TraSH) in H37Rv (ref. 42). Hypoxia is one of the major challenges

Fig. 5 | Linoleic acid promotes Ca^{2+}-dependent CTLA-4 surface trafficking. **a**,**e**, Naive $CD4^+$ T cells were stimulated with anti-CD3 and anti-CD28 antibodies in the presence of IL-2 and TGFβ for 3 days and treated with DMSO or linoleic acid (**a**) and FITC–linoleic acid (**e**). **a**, The indicated inhibitors were used to treat $CD4^+$ T_{reg} cells for 24 h. The MFI of membrane CTLA-4 levels was measured by FCM. **e**, Co-localization of FITC–linoleic acid with ER was analysed (scale bar, 1 μm). Right, pixel intensity plot for the white line. **b**,**c**, $CD4^+$ T_{reg} cells were treated with DMSO or linoleic acid for 24 h. Free cytoplasmic Ca^{2+} was assessed using FCM (**b**) and immunofluorescence analysis (**c**; scale bar, 1 μm). **d**, After 1 day of infection with the indicated Mtb strains, BMDMs were co-incubated with $CD4^+$ T_{reg} cells treated ± linoleic acid for 1 day; free cytoplasmic calcium in T_{reg} cells was assessed using FCM. **f**,**g**, $CD4^+$ T_{reg} cells were treated with DMSO or linoleic acid for 24 h. Free ER calcium was assessed using FCM (**f**) and immunofluorescence analysis (**g**; scale bar, 1 μm). Right, pixel intensity plots for the white lines. **h**, After 1 day of infection with the indicated Mtb strains, BMDMs were co-incubated with $CD4^+$ T_{reg} cells treated ± linoleic acid for 1 day; free ER calcium concentrations in T_{reg} cells were assessed by FCM. **i**, SOCE induced by thapsigargin (TG) in $CD4^+$ T_{reg} cells treated with or without linoleic acid was detected by FCM. **j**,**k**, $CD4^+$ T_{reg} cells treated with DMSO or linoleic acid for 24 h. Free ER calcium in T_{reg} cells was assessed using FCM under FCCP treatment (**j**) and immunofluorescence analysis (**k**; scale bar, 1 μm). Right, pixel intensity plots for the white lines. **l**, After 1 day of infection with indicated Mtb strains, BMDMs were co-incubated with $CD4^+$ T_{reg} cells treated with or without linoleic acid for 1 day; free ER calcium concentrations in T_{reg} cells were assessed using FCM under FCCP treatment. Data in **a**–**l** represent one experiment with three independent biological replicates ($n = 3$); mean ± s.e.m. Two-way ANOVA with Tukey's multiple-comparison test (**a**) and two-tailed unpaired Student's *t*-tests (**b**,**d**,**f**,**h**,**j**,**l**) were used for statistical analyses.

for mycobacteria in vivo[2], and significantly increased production of Rv1272c under hypoxic conditions indicated that Mtb may manipulate the level of Rv1272c to enhance bacterial survival under hypoxic in vivo conditions. The mechanism by which Mtb regulates Rv1272c expression in response to hypoxia requires further investigation.

Rv1273c/72c is functionally essential for lipid construction of the Mtb cell wall by transporting long-chain FAs[14,43]. While MsRv1273c/72c was recently characterized as an isoniazid efflux pump with putative transporting activity towards cell wall lipid precursors[21], our findings provide compelling evidence that lecithin may be its physiological substrate. We show that Rv1272c-mediated lecithin imports drive increased linoleic acid biosynthesis of Mtb, but the structure and mechanism of lecithin transporting via Rv1273c/72c are under explored. Furthermore, we identified that Rv1272c may enhance the secretion of linoleic acid from Mtb-infected macrophages mainly through the ABCG1. However, the detailed mechanism of how the linoleic acid secretion is regulated by ABCG1 or additional transporters warrants further investigation.

Linoleic acid has pro-stimulatory effects on macrophages[44,45]. Nonetheless, diverse experimental designs have indicated its potential anti-inflammatory impact as well[46]. In our Mtb-infected macrophage model, we did not observe significant effects of linoleic acid treatment on the intracellular survival of Mtb in macrophages, which may be due to the different but neutralized influence of linoleic acid to the function of macrophages through different signalling pathways. Studies on neutrophils suggest the participation of linoleic acid in airway inflammation. However, we found that deletion of Rv1272c or treatment with linoleic acid did not significantly change the percentages of neutrophils in the lung tissues of Mtb-infected mice. Furthermore, based on infection results of WT C57BL/6, *Rag1*$^{-/-}$ and *Rag1*$^{-/-}$ mice transferred with T_{reg} cells, we confirmed that Rv1272c-induced linoleic acid may not function through antimicrobial activity of innate immune cells, including macrophages or neutrophils, but promote Mtb immune evasion mediated by T_{reg} cells in vivo.

In different disease models, linoleic acid appears to have different roles in T_{reg} differentiation[47]. The most recent research on inflammatory bowel disease (IBD) indicated that in vitro linoleic acid treatments did not inhibit T_{reg} differentiation, but that in vivo linoleic acid accumulation inhibited T_{reg} differentiation by inducing macrophage infiltration and proinflammatory cytokine expression in macrophages[47]. We observed that in vitro linoleic acid treatments did not affect T_{reg} percentages under conventional differentiation conditions. Furthermore, we observed that linoleic acid interacted with ATP2a3 (ref. 39) and promoted CTLA-4 surface trafficking on T_{reg} cells under Mtb infection conditions. Thus, interaction of linoleic acid with different target proteins under specific conditions may elicit diverse regulatory functions through distinct molecular or cellular mechanisms.

It was previously reported that antigen-specific T_{reg} cells in pulmonary lymph nodes from Mtb-infected C57BL/6 mice expressed higher cell surface CTLA-4 levels[10], but underlying mechanisms were unclear. Some single nucleotide polymorphisms (SNPs) of the *CTLA4* gene have been reported to associate with TB susceptibility[8]. We showed that Mtb potentially modified the infection microenvironment as indicated by high linoleic acid concentrations to increase membrane CTLA-4 levels on T_{reg} cells via essential genes, Rv1272c, thus promoting its survival in vivo. In our study, we found that CTLA-4 on T_{reg} cells suppressed ROS production in Mtb-infected macrophages, and consequently impeded bactericidal functions by macrophages. Our findings highlight a role of membrane trafficking of CTLA-4 on T_{reg} cells in the immune evasion of Mtb. However, future in-depth studies are required to delineate these complex mechanisms.

Divalent Ca^{2+} cation is a crucial T cell signalling mediator[33]. Oleic acid suppresses SERCA2 (ATP2A2) expression to inhibit $CD4^+$ T_{reg} differentiation[48]. Concurrently, elevated intracellular Ca^{2+} enhances naive $CD4^+$ T cell sensitivity to T_{reg}-polarizing signals[49]. We found that linoleic acid promoted MAM formation via ATP2a3, facilitating ER-to-mitochondria Ca^{2+} transfer and ER Ca^{2+} depletion. This triggered stromal interaction molecule 1 (STIM)-mediated SOCE, elevating cytosolic Ca^{2+} and inducing Ca^{2+}-dependent CTLA-4 surface translocation in T_{reg} cells. However, the detailed mechanism underlying the impact of linoleic acid on mitochondria MAM formation in T_{reg} cells will be assessed in future.

The rapid emergence of drug resistance necessitates novel therapeutic strategies against TB. Immune checkpoints, including programmed death-1 (PD-1), CTLA-4 and T cell immunoglobulin mucin

Fig. 6 | Linoleic acid interacts with ATP2a3 to promote Ca^{2+}-dependent CTLA-4 surface trafficking. **a**, Co-immunoprecipitation was used to detect the interaction between linoleic acid and ATP2a3 in splenic cells. **b**, SPR assay of the direct interaction of linoleic acid and ATP2a3. **c**, ATPase activity of ATP2a3 treated with or without linoleic acid was detected using ELISA in vitro. **d**, Naive $CD4^+$ T cells were stimulated with anti-CD3 and anti-CD28 antibodies in the presence of IL-2 and TGFβ for 3 days and treated with or without linoleic acid. Immunofluorescence data show Hoechst (blue), Mito-Traker (green) and ER-Traker (magenta) staining in $CD4^+$ T_{reg} cells transfected with *Atp2a3* targeting siRNA or control siRNA. Scale bar, 1 μm. Pixel intensity plots for the white lines. **e**, Naive $CD4^+$ T cells were stimulated with anti-CD3 and anti-CD28 antibodies in the presence of IL-2 and TGFβ for 3 days and treated with DMSO or linoleic acid. SOCE induced by TG in $CD4^+$ T_{reg} cells transfected with *Atp2a3*-targeting siRNA or control siRNA and treated with or without linoleic acid was detected by FCM. **f**, MFI of membrane CTLA-4 levels in $CD4^+$ T_{reg} cells transfected with *Atp2a3*-targeting siRNA or control siRNA and treated with or without linoleic acid were measured by FCM. **g**,**h**, After 1 day of infection with indicated Mtb strains, BMDMs were co-incubated with $CD4^+$ T_{reg} cells transfected with *Atp2a3*-targeting siRNA or control siRNA and treated with or without linoleic acid for 1 day; the MFI of membrane CTLA-4 levels in $CD4^+$ T_{reg} cells was measured by FCM (**g**). The bacterial burdens in BMDMs were measured at 2 days after infection (**h**). **i**,**j**, *ATP2a3*$^{loxp/+}$ or *ATP2a3*$^{loxp/+}$*Foxp3*^{Cre} mice treated with or without LA were aerosol infected with approximately 200 c.f.u. per mouse of indicated Mtb strains for 4 weeks. The MFI of membrane CTLA-4 levels in $CD4^+$ T_{reg} cells isolated from lung tissues were measured by FCM (**i**). Bacterial burdens in mouse lungs were measured using c.f.u. assay (**j**). Data in **a**–**j** represent one experiment with three independent biological replicates ($n = 3$); mean ± s.e.m. Two-tailed unpaired Student's *t*-tests (**c**,**f**) and two-way ANOVA with Tukey's multiple-comparison test (**g**–**j**) were used for statistical analyses.

https://doi.org/10.1038/s41564-025-02140-2

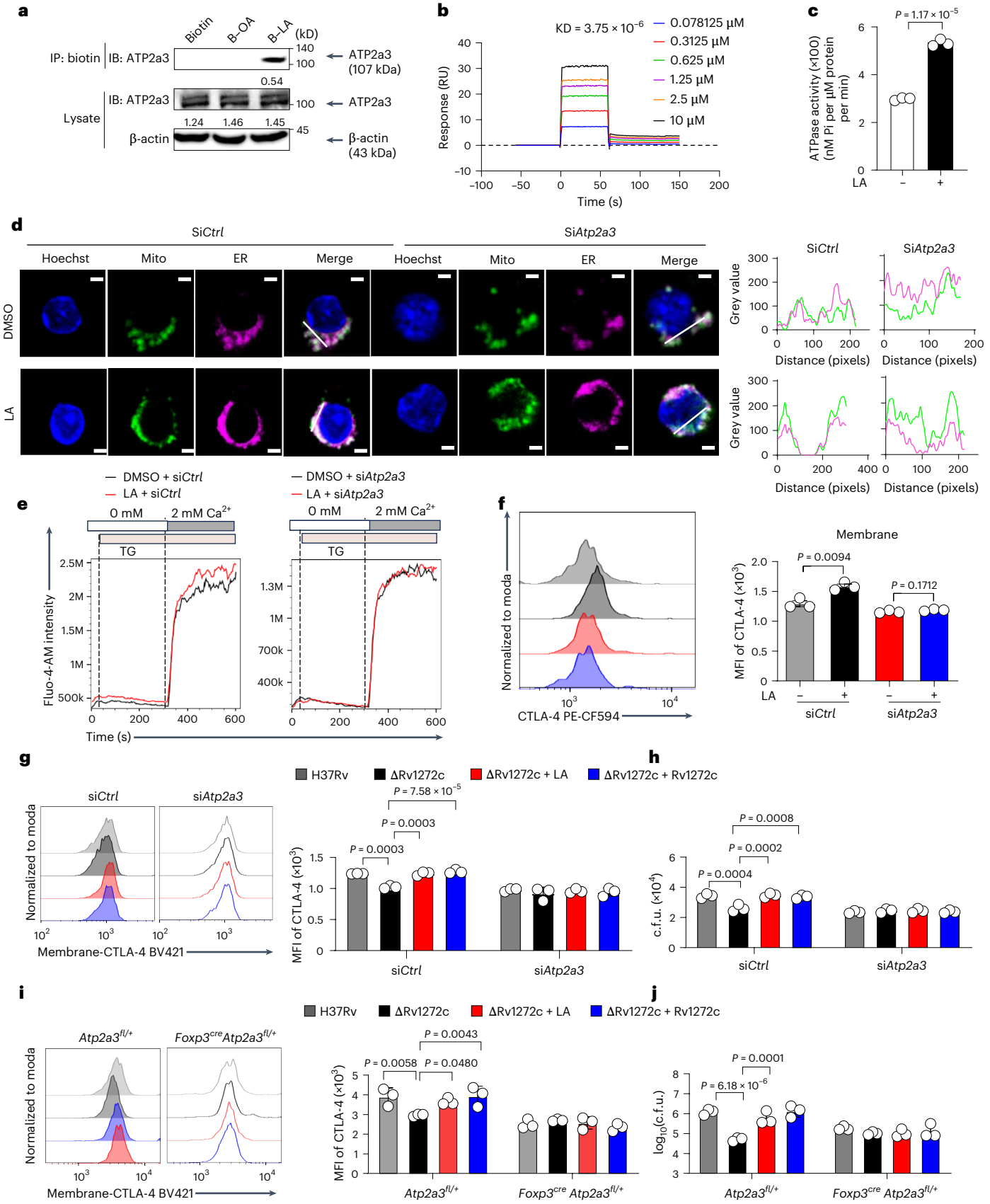

domain-containing-3 (TIM3), serve as key regulators of T cell immunity and are used in routine cancer therapy at present[50]. However, *PD-1*$^{-/-}$ mice die very rapidly after Mtb infection compared with WT mice[51], and numerous clinical cases of TB reactivation after treatment with anti-PD-1 antibody have been reported[52], indicating the increased risk or severity of TB with PD-1 blockade. TIM3 blockade conferred only minimal reduction in lung bacterial load ($\log_{10}$(colony-forming units (c.f.u.)) < 0.5) versus isotype controls in Mtb-infected C57BL/6J mice[53]. We observed that blocking T_{reg} cells or CTLA-4 shows therapeutic potential.

Our study still has several limitations. Although CTLA-4 blockade shows promise in enhancing bacterial control, its efficacy and safety alongside first-line TB drugs require systematic evaluation in animal models and clinical trials. Furthermore, clinical data linking our findings to TB progression in patients are lacking, necessitating future translational studies.

Collectively, we reveal a critical immunosuppressive mechanism in TB, in which CTLA-4 upregulation on T_{reg} cells hinders intracellular clearance of Mtb in macrophages (Extended Data Fig. 10). Our findings show that blocking T_{reg} or CTLA-4 enhances host anti-TB immunity, suggesting its potential as a therapeutic strategy pending future validation in TB treatment.

Methods

Ethics consideration

All animal experiments were approved by the Animal Experiment Administration Committee of Tongji University School of Medicine (TJAA06520101) and followed the National Institutes of Health Guidelines for the Care and Use of Laboratory Animals.

Bacterial strains

Bacterial strains used in this study were described in Supplementary Table 3. Mycobacterial strains were cultured in Middlebrook 7H9 broth (BD Biosciences, 271310) plus oleic acid–albumin–dextrose–catalase (OADC, 10%) (BD Biosciences, 212351) and tyloxapol (0.05%) (MedChemExpress, HY-B1068). This is referred to as standard 7H9–OADC–glycerol–tyloxapol media. Propionate was supplemented at 0.1 mM. Antibiotics penicillin (Sigma, P4333), kanamycin (MedChemExpress, HY-16566), Zeocin (Invitrogen, R25001) and hygromycin B (Thermo Fisher, 10687010), all at 50 μg ml^{-1}, were added for strain selection. For linoleic acid or lecithin detection, Mtb was cultured in standard 7H9–OADC–glycerol–tyloxapol medium with or without 100 μM lecithin (MedChemExpress, HY-B2235).

Strains were cultured to mid-log phase (optical density at 600 nm ($OD_{600\,nm}$) = 0.6). c.f.u. ml^{-1} was determined by plating serial dilutions on 7H10 agar and enumerating colonies after incubation at 37 °C for 1 month. Bacterial aliquots were prepared in glycerol (20%) and Middlebrook 7H9 medium, stored at −80 °C and used in assays (macrophage and mouse infections, western blotting (WB)).

Wayne's in vitro hypoxia model[2]

H37Rv was grown to mid-log phase ($OD_{600\,nm}$ ~0.6). For aerobic conditions, 4 ml of the protein-free liquid medium in the 20-mm screw-capped culture tubes was inoculated with 0.4 ml of the culture and incubated at 37 °C in a shaker–incubator set rotating at 180 rpm. For hypoxic conditions, 8 ml of medium was inoculated with 0.8 ml of identical culture in the tightly capped tubes, placed on a shaker–incubator set rotating at 70 rpm and incubated at 37 °C to avoid perturbation of the surface. After 14 days of incubation, 4-ml cultures under aeration or hypoxia were individually collected for western blotting.

BMDM culture conditions and siRNA-mediated gene interference

BMDMs derived from bone marrow cells of 6–8-week-old female C57BL/6 mice in vitro in the presence of macrophage colony-stimulating factor (M-CSF; ABclonal, RP01216) at 20 ng ml^{-1} were cultured in RPMI 1640 (Thermo Fisher, C11875500) supplemented with 10% (v/v) FBS and 1% (v/v) penicillin–streptomycin and incubated for 6 days (37 °C in 5% CO_2), with the medium changed every 72 h. All cells were routinely tested for contamination by mycoplasma.

Transfection experiments were performed according to the manufacturer's instructions. The siRNA in OptiMEM (Invitrogen, 31985070) was mixed with Lipofectamine RNAiMAX Transfection Reagent (Invitrogen, 13778030) at room temperature for 15 min. BMDMs plated in 6-well or 96-well plates were treated with siRNA for 6 h before incubation in complete media for the specified time. The efficiency of transfection was evaluated by qPCR. The sequences of siRNA (GenePharma) were listed in Supplementary Table 4. The sequences of qPCR primes were listed in Supplementary Table 5.

Plasmids, antibodies and reagents

Plasmids used in this study were described in Supplementary Table 3. WB or IP reagents (dilutions are shown for WB and IP experiments): anti-SigA (BioLegend, 663205; 1:1,000), anti-Rv1272c (Gene Optimal, 1:1,000), anti-GAPDH (Sigma, G9545; 1:5,000), anti-β-actin (Sigma, A5441; 1:5,000), goat anti-rabbit IgG antibody, Peroxidase Conjugated (Sigma, AP132P; 1:5,000), HRP-conjugated goat anti-mouse IgG (H + L) (ABclonal, AS003; 1:5,000), anti-SERCA3 monoclonal antibody (Proteintech Group, 1A2C2; 1:1,000) and streptavidin magnetic beads (MedChemExpress, HY-K0208).

Immunostaining reagents used were as follows: Endoplasmic Reticulum-Tracker Red (glibenclamide BODIPY TR) (Thermo Fisher, E34251; 1:1,000), Hoechst 33342 (Thermo Fisher, 62249; 1:1,000), rabbit polyclonal anti-ATP2a3 (Affinity Biosciences, DF15345; 1:200), goat anti-rabbit IgG (H + L) cross-adsorbed secondary antibody, Alexa Fluor 568 (Thermo Fisher, A-11011; 1:1,000), Armenian Hamster monoclonal CTLA-4 antibody (1B8; DyLight 594; Novus, NBP1-41000DL594), PKH26 (Sigma, PKH26 GL) and linoleic acid–FITC (XI'an ruixi Biological Technology).

FCM reagents used were as follows: anti-CD45 antibody (eBioscience, 30F11; 1:200), anti-CD3e (eBioscience, 145-2C11; 1:200), anti-CD4 (Biolegend, GK1.5; 1:200), anti-T-bet (Invitrogen, 4B10; 1:100), anti-CD25 (Invitrogen, PC61.5; 1:200), anti-CD8a (Invitrogen, 53-6.7; 1:200), anti-FOXP3 (Invitrogen, FJK-16S; 1:100), anti-CD152 (Biolegend, UC10-4B9; 1:200), I-Ab ESAT-61-20 Tetramer-PE (MBL, TS-M707-1; 1:50), anti-Ly-6G (BD Biosciences, 562737; 1:200), Reactive Oxygen Species Assay Kit (Beyotime, S0033M), fixation and permeabilization kit (BD Biosciences, 554714) and cell stimulation cocktail (plus protein transport inhibitors) (500×) (Thermo Fisher, 00-4975-93).

MAX Deluxe mouse IL-10 (Biolegend, 431414), mouse TGFβ1 precoated enzyme-linked immunosorbent assay (ELISA) kits (DAKEWE, DKW12-2710-048) and LEGEND MAX mouse IFNγ ELISA kit (Biolegend, 430807) were used.

Inhibitors used were as follows: NAC (MedChemExpress, catalogue number HY-B0215), 3-MA (MedChemExpress, catalogue number HY-19312), Z-VAD (MedChemExpress, catalogue number HY-16658B), AGHS (MedChemExpress, catalogue number HY-B1041), BafA1 (MedChemExpress, catalogue number HY-100558), FCCP (Sigma, C2920), halopemide (MedChemExpress, HY-119093), PP1 (MedChemExpress, HY-13804) and Thapsigargin (MedChemExpress, HY-13433).

Mouse strains

B6.Cg-*Thy1*^{a} Tg (CD2-Tcra, -Tcrb) 27Glkm/J (C7 TCR tg.CD90.1) mice (strain number 035728; RRID: IMSR_JAX:035728), which express a T cell receptor specific for the immunodominant Mtb antigen ESAT-6 from the human CD2 T cell promoter, were purchased from The Jackson Laboratory. *Ctla4*-floxed mice, *Atp2a3*-floxed mice, F*oxp3*^{Cre} mice and *Rag1*$^{-/-}$ mice were purchased from Cyagen. F*oxp3*^{CreERT2} transgenic mice were provided by Q. Zou (Shanghai Jiao Tong University). The *Ctla4*-floxed mice were crossed with *Foxp3*^{CreERT2} transgenic mice to produce age-matched *Ctla4*$^{fl/+}$*Foxp3*^{CreERT2} mice. The *Atp2a3*-floxed mice

were crossed with *Foxp3*^{Cre} transgenic mice to produce age-matched *Atp2a3*$^{fl/+}$*Foxp3*^{Cre} mice. Foxp3^{DTR} mice were purchased from Shanghai Model Organisms Center (NM-KI-190046). All genetic models were of the C57BL/6 background. All mice were bred in specific pathogen-free conditions at the Shanghai Pulmonary Hospital Laboratory Animal Center (temperature between 20 °C and 26 °C, relative humidity between 50% and 60%, light intensity in the feeding room 15–20 lx with 12 h:12 h light:dark cycle) and fed with 25 kGy irradiated feed (SLAC, P1101F) in accordance with hospital guidelines.

CRISPR KO library design and construction

For in vivo CRISPR KO screening, we designed an single guide RNA (sgRNA) library that targeted random positions along the genome of Mtb strain H37Rv. Briefly, the length of each sgRNA sequence is 21 nucleotides, and the sgRNAs targeting the non-template and template strands of ORFs, rRNAs, tRNAs and noncoding RNAs were all selected. The sgRNAs that targeted ORFs were designed within the first 50% of the coding sequence as much as possible. Finally, a total of 79,339 sgRNAs were synthesized by on-chip oligo synthesis. Then the oligonucleotide library was amplified and purified by gel extraction. The PCR products were cloned into BsmBI-digested pYC1446 through Golden Gate Assembly to generate a CRISPR KO plasmid library.

Cells carrying pYC1759 were grown in 400 ml containing 0.05% Tween 80, 0.2% glycerol, OADC and 25 μg ml^{-1} kanamycin in 7H9 medium in roller bottles at 37 °C for 10 days to 15 days. Competent cells were prepared and transformed with the CRISPR KO plasmid library via electroporation. The recovered cells were collected at 3,700*g* after centrifugation for 10 min and smeared on 7H10 agar plates (15 cm × 15 cm) supplemented with kanamycin, Zeocin and 100 ng ml^{-1} ATc. After 21 days of growth, colonies were scraped from each plate through 7H9 medium and gently vortexed. The KO libraries were obtained and then confirmed by using genomic DNA extraction and subsequent PCR and sequencing analysis.

In vivo screening and genomic DNA extraction

The in vivo genome-wide CRISPR KO screening was performed in the C57BL/6 mice, with five biological replicates for infection. Female C57BL/6 mice, 6–8 weeks old, were infected through an aerosol method with approximately ~1 × 10^7 c.f.u. of CRISPR KO library strain for 4 weeks at the biosafety level 3 laboratory. The remaining bacterial solution for infection was coated on the 7H10 plates with three biological replicates and incubated for 3 weeks; all clones were scraped off the plate and used for the DNA extraction as the uninfected controls. After 4 weeks of infection, the infected mice were euthanized humanely and whole lungs were collected, homogenized in 1 ml of PBS and coated on the 7H10 plates. After incubation for 3 weeks, all clones were scraped off the plate and collected for the following DNA extraction.

EZ-10 Spin Column Bacterial Genomic DNA Isolation Kit was used to extract genomic DNA according to the manufacturer's instructions. Then the sgRNA-encoding region was amplified by PCR by using genomic DNA as a template. Primers for PCR amplification are described in Supplementary Table 5. Each 50-μl reaction solution contained a 50-ng template and I-5 2X Hi-Fi PCR Master Mix (MCLAB); eight reactions were detected in each library. The amplification conditions were initial denaturation at 98 °C for 2 min and denaturation at 98 °C for 10 s for 18 cycles, annealing at 64 °C for 15 s and extension at 72 °C for 15 s, and a final extension at 72 °C for 5 min. A two-step PCR amplification of sgRNA barcodes was then performed on the CRISPR KO library, and 242-bp PCR fragments were finally obtained.

Sequencing library preparation and sequencing

The obtained PCR fragments from the previous step were sent for sequencing library preparation and sequencing. In short, End Prep Mix was used for end repair, 5′ phosphorylation and dA-tailing in one reaction of purified PCR fragments, followed by T-A ligation to add adaptors to both ends. The sample purification beads were used to purify the adaptor-ligated DNAs, and P5 and P7 primers were used for PCR amplification of eight cycles. The PCR products were cleaned with sample purification beads, verified by Qsep100 and quantified by Qubit3.0 Fluorescence (Invitrogen). According to the manufacturer's instructions (Illumina), libraries with different indexes were multiplexed and loaded onto the Illumina NovaSeq instrument to adopt 2 × 150 paired-end sequencing.

Sequencing data analysis

Sequences of sgRNAs were obtained from sequencing data by using an in-house script. Alignment to the library and the counts of the sgRNAs were performed using MAGeCK (v0.5.7)[54]. The obtained count matrix was then analysed by the MAGeCK robust rank analysis method. To obtain reliable negative screening hits, the sgRNAs with an average read count of less than 50 in the original library for screening were removed, and the read counts were normalized relative to the reads of non-targeting control sgRNAs in each sample. Genes with $\log_2$ fold change (FC) lower than −1 and *P* value lower than 0.05 were considered essential. The MAGeCK gene summary output results can be found in Supplementary Table 1. Figures were created using the ggplot2 package in R (v4.2.2).

Mice infections

Female C57BL/6, *Foxp3*^{DTR}, *Ctla4*$^{fl/+}$, *Ctla4*$^{fl/+}$*Foxp3*^{CreERT2}, *Atp2a3*$^{fl/+}$, *Atp2a3*$^{fl/+}$*Foxp3*^{Cre} and *Rag1*$^{-/-}$ mice, 6–8 weeks old, were randomly divided into cages and aerosol infected with different H37Rv strains (~200 c.f.u.) for 1 day or 4 weeks (Glas-Col inhalation system) at the biosafety level 3 laboratory. All mice were age and weight matched. Mice were then provided with water containing either vehicle (0.3% xanthan gum in deionized water) or linoleic acid (0.5% in 0.3% xanthan gum in deionized water) for 4 weeks. The xanthan gum solution was used to equalize solution texture according to a previous study[55]. Solutions were replaced daily.

The following reagent doses were given to mice, along with appropriate IgG controls or diluents: (1) anti-CTLA-4 monoclonal antibody (BioXcell, BE0131) at 500 μg per mouse, intraperitoneally provided at 4, 8, 12, 16, 20 and 24 days postinfection (dpi); (2) diphtheria toxin (DT) (Sigma-Aldrich, D0564) at 1 μg per mouse, at 4, 8, 12, 16, 20 and 24 dpi; (3) 1 mg tamoxifen (Sigma, T5648) in corn oil, at 4, 8, 12, 16, 20 and 24 dpi.

Mice were euthanized humanely at 1 day or 4 weeks after infection. Lung tissue and serum samples were collected. Serum was used for linoleic acid detection by ultra-performance liquid chromatography (UPLC), and TGFβ1, IL-10 or IFNγ levels were determined by ELISA. Approximately 50% of lung tissue was dissociated to determine different T cell percentages and detect bacterial burdens or linoleic acid levels.

For histology, approximately 50% of lung tissues from infected mice (4 weeks) were fixed in 4% neutral-buffered paraformaldehyde for 1 day and paraffin embedded. Sections (4–7 μm) were stained with haematoxylin and eosin (H&E) or Ziehl–Neelsen (for acid-fast bacilli) stains. An automated whole-slide scanning device (3DHISTECH, Sysmex) was used to record images.

GC–MS metabolomics analyses

Metabolomics analyses on Mtb-infected BMDM culture supernatants (filtered using 0.22-μm pore membranes (Millipore)) were performed.

For metabolite extraction, 50 μl of sample was transferred into a 2-ml EP tube, and 1 ml of acetonitrile:isopropanol:water (3:3:2, v/v/v) mixed solution (−20 °C) was added. Vortex oscillation was performed for 30 s. Then, room temperature ultrasound for 5 min and 12,000 rpm centrifugation were performed for 2 min; 500 μl of supernatant solution was taken and added into a new 2-ml EP tube. The vacuum concentrator was concentrated to dryness (8–10 h), and the remaining

supernatant was placed in a refrigerator at −80 °C for backup. Then, 80 µl of 20 mg ml^{-1} MEOX solution was added for redissolution, and vortex vibration for 30 s and incubation at 60 °C for 60 min were performed. Finally, 100 µl BSTFA-TMCS (99:1) reagent was added, followed by a reaction at 70 °C for 90 min and centrifugation at 14,000 rpm for 3 min, and 90–100 µl of supernatant was added into the detection bottle. Samples were placed in sealed cuvettes to be tested and processed for GC-TOF upper detection.

Gas chromatography was performed on a DB-5MS capillary column (30 m × 250 µm i.d., 0.25 µm film thickness; Agilent J & W Scientific) to separate the derivatives at a constant flow of 1 ml min^{-1} helium. Then, 1 µl of sample was injected in split mode in a 1:10 split ratio by the autosampler. The injection temperature was 280 °C. The temperature of the transfer line ion source was 320 °C and 230 °C, respectively. The programmes of temperature rise were followed by an initial temperature of 50 °C for 0.5 min, 15 °C min^{-1} rate up to 320 °C and staying at 320 °C for 9 min. Mass spectrometry was performed using a full scan method with a scan rate of 10 spec s^{-1}, electron energy of −70 V and a solvent delay of 3 min. Raw data analysis, including peak extraction, baseline adjustment, deconvolution, alignment and integration, was performed using Chroma TOF (v.4.3x, LECO) software. The LECO-Fiehn Rtx5 database54 and the updated Fiehn library database57 were used for metabolite identification by matching mass spectra and retention indices. Finally, peaks detected in less than half of QC samples or with relative standard deviation > 30% in QC samples were removed.

Linoleic acid assays

To quantify linoleic acid, GC–MS was conducted. Samples were resuspended in 450 µl of extracting solution ($V_{\text{Isopropanol}}$:$V_{n\text{-hexane}}$ = 2:3, containing 0.21 mg l^{-1} internal standard), treated with ultrasound for 10 min (incubated in ice water) and then centrifuged for 15 min at 12,000*g* at 4 °C. The supernatant was transferred into fresh 2-ml EP tubes. Then 500 µl of extract solution ($V_{\text{Isopropanol}}$:$V_{n\text{-hexane}}$ = 2:3, containing 0.21 mg l^{-1} internal standard) was added to the remaining samples, and the mixture was vortex mixed for 30 s; steps 2 and 3 were repeated. The supernatants from step 5 and step 3 were combined and vortexed for 30 s. Subsequently, 800 µl of the combined supernatant was taken and nitrogen blow dried. Then, 500 µl of methanol:trimethylsilyl diazomethane solution (1:2) was added, allowed to stand at room temperature for 30 min and nitrogen blow dried. Subsequently, 160 µl of *n*-hexane was added, redissolved and centrifuged for 1 min at 12,000*g*. The supernatant was transferred into a fresh vial for GC–MS analysis.

GC–MS analysis was performed using an Agilent 7890B gas chromatograph system coupled with an Agilent 5977B mass spectrometer. The system used a DB-FastFAME capillary column. A 1 µl aliquot of the analyte was injected in split mode (5:1). Helium was used as the carrier gas, the front inlet purge flow was 3 ml min^{-1} and the gas flow rate through the column was 46 psi with constant pressure. The initial temperature was kept at 75 °C for 1 min, raised to 200 °C at a rate of 50 °C min^{-1} for 15 min, raised to 210 °C at a rate of 2 °C min^{-1} for 1 min, and raised to 230 °C at a rate of 10 °C min^{-1} for 16.5 min. The injection, transfer line, quad and ion source temperatures were 240 °C, 240 °C, 230 °C and 150 °C. The energy was −70 eV in electron impact mode. The mass spectrometry data were acquired in SIM mode after a solvent delay of 7 min.

Lecithin assays

To quantify lecithin, ultra-high-performance liquid chromatography–MS/MS (UHPLC–MS/MS) was conducted. Samples were resuspended in 50 µl of a 1:1 isopropanol:methanol HPLC-grade solution before the analyses. The UHPLC separation was carried out using an Agilent 1290 Infinity II series UHPLC System (Agilent Technologies), equipped with an ACQUITY UPLC BEH C18 (150 × 2.1 mm, 1.7 µm, Waters). The mobile phase A was 10 mM ammonium formate and 0.1% formic acid in water, the mobile phase B was acetonitrile and the moblie phase C was isopropanol. The autosampler temperature was set at 4 °C, and the injection volume was 1 µl. The column temperature was set at 35 °C.

An Agilent 6460 triple quadrupole mass spectrometer (Agilent Technologies), equipped with an AJS electrospray ionization interface, was applied for assay development. Typical ion source parameters were as follows: capillary voltage = +4,000/−3,500 V, nozzle voltage = +500/−500 V, gas (N_2) temperature = 300 °C, gas (N_2) flow = 5 l min^{-1}, sheath gas (N_2) temperature = 250 °C, sheath gas flow = 11 l min^{-1} and nebulizer = 45 psi.

The MRM parameters for each of the targeted analytes were optimized using flow injection analysis, by injecting the standard solutions of the individual analytes, into the API source of the mass spectrometer. Several most sensitive transitions were used in the MRM scan mode to optimize the collision energy for each Q1–Q3 pair. Among the optimized MRM transitions per analyte, the Q1–Q3 pairs that showed the highest sensitivity and selectivity were selected as 'quantifier' for quantitative monitoring. The additional transitions acted as 'qualifier' for the purpose of verifying the identity of the target analytes. Agilent MassHunter Work Station Software (B.08.00, Agilent Technologies) was used for MRM data acquisition and processing.

Mycobacteria strain construction

Rv1272c KO in the H37Rv strain was generated using CRISPR–NHEJ-assisted genome editing[11]. The H37Rv strain, harbouring the helper pNHEJ-*recX-sacB* plasmid, was grown in 10 ml 7H9 medium plus tyloxapol (0.05%), glycerol (0.2%), OADC and kanamycin (25 µg ml^{-1}) until saturation at $OD_{600\ nm}$ ~1.0. Then, 1 ml or 2 ml was inoculated into 100 ml of complete 7H9 broth plus kanamycin (25 µg ml^{-1}) and incubated (rolling at 75 rpm) at 37 °C for 5–7 days. When the $OD_{600\ nm}$ reached ~0.8, 10 ml of a sterilized glycine stock solution (15%) was added and incubation continued (37 °C with rolling) for 20–24 h.

After competent H37Rv cell preparation, approximately 300 ng of a Cas9-sgRNA plasmid (pYC1876), inserted with sgRNA targeting Rv1272c (sgRNA1: gcccggctgctcaacctcaccgt; sgRNA2: ggccagcaccgccaccatgg), was mixed with competent cells. Electroporation settings were 25 µF, 2.5 kV and 1,000-Ω resistance. Cells were then cultured in 7H9 broth (1 ml) plus OADC and incubated for 48 h at 37 °C to permit high densities and mimic the stationary phase. Next, transductants were plated onto 7H10 agar plus OADC (10%) and hygromycin (50 µg ml^{-1}) and cultured at 37 °C for approximately 3 weeks until colonies appeared. Antibiotic-resistant clones were randomly selected and verified using colony PCR, sequencing to confirm *rv1272c* deletion. The complementation plasmid for the Rv1272c was generated by ligating the PCR products using Rv1272c-specific primers into the episomal vector, pVV16 with hsp60 promoter. The resulting plasmid was transformed into the H37RvΔRv1272c strain and plated on a 7H10 plate containing Zeocin (Invitrogen, R25001) at 50 µg ml^{-1}. Positive integrants carrying the required insert were screened by colony PCR and validated by immunoblot analyses. Primers for PCR identification are described in Supplementary Table 5.

Growth curves

Mid-log phase mycobacteria were cultured in standard 7H9–OADC–glycerol–tyloxapol media and antibiotics. Growth curves were generated on a Bioscreen C growth curve instrument (Labsystems Oy) using 100-well honeycomb plates (Labsystems Oy). Approximately 200 µl of a bacterial suspension, adjusted to a similar density, was added to wells and cultured with shaking at 37 °C. $OD_{590\ nm}$ was measured daily. H37Rv cultures were incubated for 2 weeks. Three independent experiments were performed in triplicate.

Total lipid extraction and TLC

Cultures were grown in 7H9 broth in a volume of 50 ml to an $OD_{600\ nm}$ of 0.8. Cultures were pelleted and resuspended in 2:1 methanol–chloroform and left at 4 °C overnight. Samples were spun down, and

the supernatant was transferred to a glass beaker. The pellet was resuspended in 1:1 methanol–chloroform and left at room temperature for an hour. Samples were spun down, and the supernatant was removed. The process was repeated again with 1:2 methanol–chloroform. All three fractions were pooled, and the methanol and chloroform were allowed to evaporate overnight in a fume hood. The total lipid pellet was weighed, and 300 µg of total lipid was spotted onto a TLC plate. The plate was resolved in a mobile phase of 9:1 petroleum ether–diethyl ether. Lipid spots were revealed by spraying the plate with a solution of 3% cupric acetate in 8% phosphoric acid followed by baking at 140 °C.

Intracellular bacterial growth

BMDMs were infected with Mtb at a multiplicity of infection (MOI) = 5. At 3 h, 24 h or 48 h postinfection, cells were lysed in Triton X-100 (0.2%) and 10-fold serial dilutions were plated onto 7H10 agar plus ADC (10%) and incubated at 37 °C. Colonies were counted after 1 month at 37 °C in 5% CO_2 (ref. 2), after which a linear Mtb intracellular survival scale was generated.

IP and WB

Spleen cells were isolated from spleens of 6–8-week-old female C57BL/6 mice. Cell lysis buffer (plus a 1% protease-inhibitor cocktail (Sigma, P8340)) was used to lyse cells for WB and IP (Beyotime, P0013). After incubation on ice for 30 min, lysates were centrifuged at 12,000*g* for 10 min at 4 °C to clear cellular debris. Next, a 50-µl clarified lysate aliquot was prepared as a total cell lysate sample. To confirm linoleic acid interactions with ATP2a3, remaining cell lysates were incubated with biotin, oleic acid–biotin or linoleic acid–biotin (100 µM) (Bootech Bioscience) for 180 min at 4 °C, and then incubated overnight with streptavidin magnetic beads at 4 °C for IP the next day.

For WB, Mtb or T cell extracts were denatured in 1 × sodium dodecyl sulfate (SDS) buffer and electrophoresed on 10% or 12% SDS-polyacrylamide gels. Gels were then transferred to nitrocellulose membranes, after which membranes were blocked, washed three times and incubated with primary anti-SigA, anti-Rv1272c and anti-ATP2a3 antibodies (dilution = 1:1,000) and an anti-GAPDH antibody (1:5,000). A horseradish peroxidase-conjugated goat anti-rabbit or anti-mouse polyclonal secondary antibody was then used (1:5,000). After membrane washing, enhanced chemiluminescence (Thermo Fisher, C500044) was used to highlight protein bands.

Pull-down in vitro

HIS-ATP2a3 (2 µg, Shanghai Sincere Biotech) was added to cytosolic buffer (40 mM HEPES pH 7.4, 0.1% Triton X-100, 10 mM NaCl, 150 mM KCl, 2.5 mM $MgCl_2$, 1 mM GDP) containing 10 mM of biotin, biotin–linoleic acid and incubated with streptavidin magnetic beads for 6 h at 4 °C. The beads were centrifuged, washed with cytosolic buffer and denatured by heating at 100 °C in loading buffer. Proteins were separated by SDS–PAGE gel and assayed by Coomassie staining and immunoblotting.

SPR

The interaction between ATP2a3 and linoleic acid was analysed by OpenSPR (Nicoya Lifesciences) using a COOH-functionalized sensor chip. The chip was installed according to the manufacturer's protocol and primed at a maximum flow rate (150 µl min^{-1}) with PBST buffer (pH 7.4). Upon baseline stabilization, the sample loop was flushed with buffer and purged. After signal return to baseline, the flow rate was reduced to 30 µl min^{-1}. The chip surface was activated with freshly prepared EDC–NHS solution (1:1 ratio).

A 200-µl ligand diluted in activation buffer was run for 4 min. When binding was stabilized, the sample ring was rinsed with buffer. Then, 200 µl of blocking solution was applied, and the sample ring was rinsed with the buffer solution and dried using air. The baseline was monitored for 5 min to ensure stability. The flow rate was increased to 150 µl min^{-1} and appropriate regeneration buffer was injected to remove the analyte. The analyte was diluted with buffer solution, the concentration was shown in the experimental results, and the sample was taken at 30 µl min^{-1}. The binding time of the ligand and analyte was 120 s, and the natural dissociation was 300 s. The analysis software used for the experimental results is TraceDrawer (Ridgeview Instruments AB), and the the analytical method was the one to one analytical model.

qPCR analysis

qPCR analysis was performed using gene-specific primers (Supplementary Table 4). Total RNA was extracted with 1 ml of Trizol reagent according to the manufacturer's instructions (Thermo Fisher). Total RNA (1 µg) was used for complementary DNA synthesis with the ReverTra Ace qPCR RT kit (Toyobo). qPCR was performed using the SYBR RT–PCR kit (Toyobo) in an LC480 thermocycler (Roche). The $2^{-\Delta\Delta Ct}$ method was adopted to analyse relative gene expression, which was normalized to the expression of *sigA* (*Mtb*H37Rv) or *gapdh* (mice). qPCR data were collected from at least three independent experiments with three technical replicates per experiment.

T cell purification and transduction

Mouse naive $CD4^+$ T cells were activated in vitro. Naive $CD4^+$ T cells were isolated from spleens of 6–8-week-old female C57BL/6 mice using a naive $CD4^+$ T cell isolation kit (Biolegend, 480040). Purified naive $CD4^+$ T cells were activated in vitro for 24 h using 5 µg ml^{-1} of plate-bound anti-CD3 (BioXcell, BE0001-1) and 1 µg ml^{-1} of anti-CD28 (Peprotech, 37.51) antibodies.

ESAT-$6_{4–17}$-specific $CD4^+$ T cells were activated in vivo. After 24 h of intravenous injection of peptide ESAT-$6_{4–17}$ into 6–8-week-old female C7 TCR tg.CD90.1 mice, spleen cells from C7 TCR tg.CD90.1 mice were pooled and enriched for ESAT-$6_{4–17}$: I-A^b tetramer-binding $CD4^+$ T cells with magnetic beads and columns.

Activated $CD4^+$ T cells were transfected with *Atp2a3*-targeting siRNAs or control siRNAs with the ProteanFect Max Mouse Immunocyte Transfection Kit (Nanoportal Biotech, PT03). Cells were then cultured with mouse IL-2 (10 ng ml^{-1}; Peprotech, 212-12) and recombinant mouse TGFβ1 protein (R&D SYSTEMS, 7666-MB; 5 ng ml^{-1}) for 48 h. Successfully transfected Foxp3-positive $CD4^+$ T cells were used in functional analyses.

T cell differentiation and stimulation in vitro

WT $CD4^+$ T cells were activated in vitro. Naive $CD4^+$ T cells isolated from spleens of 6–8-week-old female C57BL/6 mice were stimulated with 5 µg ml^{-1} of plate-bound anti-CD3, 1 µg ml^{-1} of an anti-CD28 antibody, 20 ng ml^{-1} human IL-2 (Peprotech, 212-12) and recombinant mouse TGFβ1 protein (5 ng ml^{-1}, R&D SYSTEMS, 7666-MB). Cells were polarized towards a Foxp3-positive $CD4^+$ T cell phenotype and treated with linoleic acid (100 µM, MedChemExpress, HY-N0729) for 48 h. Cells were then grown in complete RPMI 1640 plus FBS (10%, v/v) and penicillin–streptomycin (1%, v/v). A calcium chelator (EGTA, 3 mM, Sigma, 67-42-5), halopemide (2 µM, MedChemExpress, HY-119093), PP1 (20 mM, MedChemExpress, HY-13804) and thapsigargin (1 µM, MedChemExpress, HY-13433) were used to treat $CD4^+$ T_{reg} cells and examine if linoleic acid promoted $CD4^+$ T_{reg} cells via a corresponding signalling pathway.

Confocal microscopy

In vitro-differentiated T_{reg} cells were plated at 1×10^6 ml^{-1}, followed by staining with ER-Tracker Red (Invitrogen, E34250) and treatment with FITC-conjugated linoleic acid (linoleic acid–FITC; Xi'an Ruixi Biological Technology) for 30 min at 37 °C in the dark. Simultaneously, Hoechst 33342 nuclear stain was added (37 °C for 10 min in the dark). Samples were then visualized under confocal microscopy (Leica).

To detect the MAMs, T_{reg} cells were stained with ER-Tracker Red (Invitrogen, E34250) and MitoTracker Deep Red FM (Thermo Fisher,

M22426) in the dark for 30 min at 37 °C. Simultaneously, Hoechst 33342 nuclear stain was added (37 °C for 10 min in the dark). Samples were then visualized under confocal microscopy (Leica).

To detect the co-localization of linoleic acid and ATP2a3, T_{reg} cells were treated with linoleic acid–FITC in the dark for 30 min at 37 °C, fixed with 4% paraformaldehyde for 30 min, permeabilized with 0.1% Triton X-100 for 3 min and blocked with 3% BSA in PBS for 15 min at room temperature. Cells were subsequently stained with rabbit polyclonal anti-ATP2a3 (Affinity Biosciences, DF15345) overnight at 4 °C, followed by detection with goat anti-mouse IgG (H + L) highly cross-adsorbed secondary antibody, Alexa Fluor 568 (Thermo Fisher, A-11031). Nuclei were stained with Hoechst. Samples were visualized using a Leica confocal microscope.

T_{reg} cells were incubated with Fluo-4-AM dye (Abcam, ab112129) to report cytoplasm Ca^{2+}. Fluo-4-AM-loaded cells were washed three times in calcium-free Hank's buffer to remove extracellular calcium. Then, T_{reg} cells (approximately 1×10^6) were resuspended in 0.5 ml Hank's buffer. Nuclei were stained with Hoechst. Samples were visualized using a Leica confocal microscope.

T_{reg} cells were incubated with Mag-Fluo-4 AM (MedChemExpress, HY-D1498) to report ER Ca^{2+} as previously described[56]. The ER was loaded with indicator by incubating cells with Mag-Fluo-4 AM (20 μM, 30 min, 37 °C) in Hank's buffer, supplemented with 1% FBS. After washing and permeabilization with 10 μg ml^{-1} of saponin (Sigma, 84510) for 37 °C, 2–3 min in Ca^{2+}-free cytosol-like medium (Ca^{2+}-free CLM), cells were centrifuged (650*g*, 2 min) and resuspended in Mg^{2+}-free CLM supplemented with 375 μM $CaCl_2$ and 10 μM FCCP (Sigma, C2920). FCCP is included to inhibit mitochondrial Ca^{2+} uptake. Nuclei were stained with Hoechst. Samples were visualized using a Leica confocal microscope. Ca^{2+}-free CLM comprised 20 mM NaCl, 140 mM KCl, 1 mM EGTA, 20 mM PIPES and 2 mM $MgCl_2$, pH 7.0.

T_{reg} cells were labelled with membrane dye PKH26 (Sigma, PKH26GL). After coculture for 30 min at 37 °C, cells were collected and washed twice. The total CTLA-4 expression was determined by fixing cells in 2% paraformaldehyde for 5 min at 4 °C. Cells were washed once in PBS followed by staining with Armenian Hamster Monoclonal CTLA-4 Antibody (1B8; DyLight 594; Novus, BP1-41000DL594) in PBS containing 0.1% saponin. Cells were washed in PBS–saponin. Nuclei were stained with Hoechst. Samples were visualized using a Leica confocal microscope.

ATPase activity assay

The ATPase activities of recombinant ATP2a3 (CSB-MP727334MO, CUSABIO Technology LLC) treated with or without linoleic acid were measured using the ATPase/GTPase Activity Assay Kit (MAK-113, Sigma-Aldrich) according to the manufacturer's instruction. To measure the ATPase activities of ATP2a3 against different substrates, protein at a final concentration of 5 μM was added to the HEPES–NaCl–glycerol buffer containing 20 mM HEPES pH 8.5, 13 mM NaCl and 1% glycerol. Then, each substrate was added into the reaction mixture. ATP was supplemented in the solution with a final concentration of 2 mM to start the reaction at 37 °C for 60 min. The amount of released Pi was quantitatively measured at $OD_{650\,nm}$.

Calcium flux analyses

Differentiated $CD4^+$ T_{reg} cells were incubated with Fluo-4-AM dye (Abcam, ab112129) to report cytoplasm Ca^{2+}, while Mag-Fluo-4 AM (MedChemExpress, HY-D1498) was used to report ER Ca^{2+} as previously described[56]. ER Ca^{2+} loading was achieved by incubating cells with 20 μM Mag-Fluo-4 AM in Hank's balanced salt solution supplemented with 1% FBS for 30 min at 37 °C. After washing and permeabilization with 10 μg ml^{-1} of saponin (Sigma, 84510) for 37 °C, 2–3 min in Ca^{2+}-free CLM, cells were centrifuged (650*g*, 2 min) and resuspended in Mg^{2+}-free CLM supplemented with 375 μM $CaCl_2$ and 10 μM FCCP (Sigma, C2920) and subjected to FCM. Fluo-4-AM-loaded cells were washed three times in calcium-free Hank's buffer to remove extracellular calcium. Then, $CD4^+$ T_{reg} cells (approximately 1×10^6) were resuspended in 1 ml Hank's buffer and subjected to FCM (CytoFLEX S, Beckman Coulter). Intracellular calcium signals were simultaneously acquired. Thapsigargin was used to induce calcium release from the ER. Store-operated Ca^{2+} influx was recorded when 2 mM $CaCl_2$ was added to thapsigargin.

Co-culture assays

For co-culture assays[2], approximately 1×10^5 BMDMs per well were infected with different Mtb strains (MOI = 5). After 3 h, extracellular bacteria were removed by washing cells three times in warm PBS. Infected BMDMs were incubated at 37 °C for 21 h. Next, differentiated $CD4^+$ T_{reg} cells treated with linoleic acid or not were co-cultured with BMDMs (5×10^4 per well) for 24 h. After co-culturing, Foxp3-positive $CD4^+$ T cells, membrane and total CTLA-4 levels, and intracellular bacterial growth were determined.

For detection of membrane and total CTLA-4 levels, after co-culture of uninfected and Mtb strain-infected BMDMs (MOI = 5) and T cells treated with or without linoleic acid for 1 day, membrane and total CTLA-4 levels were measured in $CD4^+$ T_{reg} cells using FCM.

To determine intracellular bacterial growth, BMDMs were infected with Mtb strains. Intracellular bacterial c.f.u. in BMDMs were determined at indicated times. BMDMs infected with Mtb strains without co-incubation with $CD4^+$ T_{reg} cells for 2 days were used as control.

FCM

For surface marker analyses, cells were incubated in PBS plus bovine serum albumin (2%, w/v; Sigma) for 30 min on ice. For transcription factor staining, FOXP3–transcription factor staining buffers were used (eBioscience, 00-5523-00). For intracellular cytokine staining, a fixation and permeabilization kit was used (BD Biosciences, 554714). Cells for intracellular cytokine staining were activated using a cell stimulation cocktail (eBioscience, 00-4975-93). Cells were stained with surface markers, fixed and permeabilized using a fixation and permeabilization kit (BD Biosciences), and stained with anti-Foxp3 antibody (Invitrogen, FJK-16S, 1:100). Cells were washed twice and determined by FCM. For surface and total CTLA-4 expression analyses, cells were labelled with a BV421-anti-CD152/APC-anti-CD152 (Biolegend, UC10-4B9, 1:200) antibody at 4 °C for 1 h either before or after the fixation and permeabilization step to compare surface and total CTLA-4 expression[57]. ROS levels (Beyotime, S0033S) were determined by FCM. Fluorescence minus one control was used to distinguish positive and negative populations for CTLA-4 and ROS detection.

Statistical analyses

All data were analysed in Prism 9.0 software (GraphPad). Data distribution was assumed to be normal, but this was not formally tested. Data collection was randomized, and animals and samples were assigned to the various experimental groups randomly. The data collection and analysis were not performed blind to the conditions of the experiments. Statistically significant differences between two groups were determined using two-tailed unpaired Student's *t*-tests. Two-way analysis of variance with Tukey's multiple-comparison test and one-way analysis of variance with Tukey's multiple-comparison test were used when comparing two or more groups. $P < 0.05$ was deemed statistically significant. All data were taken from technical replicate averages from several independent experiments and represented by the mean ± s.e.m. No statistical methods were used to pre-determine sample sizes, but our sample sizes are similar to those reported in previous publications[2].

Reporting summary

Further information on research design is available in the Nature Portfolio Reporting Summary linked to this article.

Data availability

The metabolomics datasets for the analysis of Mtb-infected BMDM culture supernatant profiles are available in the MetaboLights database under accession number MTBLS12875. The CRISPR KO screening analysis data and the mass spectrometry data for comparative metabolomics analysis are provided as Supplementary Tables 1 and 2. Source data are provided with this paper.

Code availability

All analyses were done reproducibly using publicly available R scripts.

References

1. Chai, Q., Wang, L., Liu, C. H. & Ge, B. New insights into the evasion of host innate immunity by *Mycobacterium tuberculosis*. *Cell Mol. Immunol.* **17**, 901–913 (2020).
2. Cheng, H. et al. *Mycobacterium tuberculosis* produces D-serine under hypoxia to limit $CD8^+$ T cell-dependent immunity in mice. *Nat. Microbiol.* **9**, 1856–1872 (2024).
3. Kursar, M. et al. Cutting edge: regulatory T cells prevent efficient clearance of *Mycobacterium tuberculosis*. *J. Immunol.* **178**, 2661–2665 (2007).
4. Cardona, P. & Cardona, P. J. Regulatory T cells in *Mycobacterium tuberculosis* infection. *Front. Immunol.* **10**, 2139 (2019).
5. Zewdie, M. et al. Ex-vivo characterization of regulatory T cells in pulmonary tuberculosis patients, latently infected persons, and healthy endemic controls. *Tuberculosis* **100**, 61–68 (2016).
6. Shafiani, S., Tucker-Heard, G., Kariyone, A., Takatsu, K. & Urdahl, K. B. Pathogen-specific regulatory T cells delay the arrival of effector T cells in the lung during early tuberculosis. *J. Exp. Med.* **207**, 1409–1420 (2010).
7. Rowshanravan, B., Halliday, N. & Sansom, D. M. CTLA-4: a moving target in immunotherapy. *Blood* **131**, 58–67 (2018).
8. Liu, C. W. et al. Association of tuberculosis risk with genetic polymorphisms of the immune checkpoint genes PDCD1, CTLA-4, and TIM3. *PLoS ONE* **19**, e0303431 (2024).
9. Wang, P. H. et al. The dynamic change of immune checkpoints and $CD14^+$ monocytes in latent tuberculosis infection. *Biomedicines* **9**, 1479 (2021).
10. Shafiani, S. et al. Pathogen-specific Treg cells expand early during *Mycobacterium tuberculosis* infection but are later eliminated in response to interleukin-12. *Immunity* **38**, 1261–1270 (2013).
11. Yan, M. Y., et al. A CRISPR-assisted nonhomologous end-joining strategy for efficient genome editing in *Mycobacterium tuberculosis*. *mBio* **11**, e02364-19 (2020).
12. Vandal, O. H. et al. Acid-susceptible mutants of *Mycobacterium tuberculosis* share hypersusceptibility to cell wall and oxidative stress and to the host environment. *J. Bacteriol.* **191**, 625–631 (2009).
13. Yu, J. et al. Structure and mechanism of a mycobacterial isoniazid efflux pump MsRv1273c/72c with a degenerate nucleotide-binding site. *Nat. Commun.* **16**, 3969 (2025).
14. Martin, A. & Daniel, J. The ABC transporter Rv1272c of *Mycobacterium tuberculosis* enhances the import of long-chain fatty acids in *Escherichia coli*. *Biochem. Biophys. Res. Commun.* **496**, 667–672 (2018).
15. Bomalaski, J. S., Steiner, M. R., Simon, P. L. & Clark, M. A. IL-1 increases phospholipase A2 activity, expression of phospholipase A2-activating protein, and release of linoleic acid from the murine T helper cell line EL-4. *J. Immunol.* **148**, 155–160 (1992).
16. Schaffer, J. E. Fatty acid transport: the roads taken. *Am. J. Physiol. Endocrinol. Metab.* **282**, E239–E246 (2002).
17. Ekim Kocabey, A. & Schneiter, R. Human lipocalins bind and export fatty acids through the secretory pathway of yeast cells. *Front. Microbiol.* **14**, 1309024 (2023).
18. Cavelier, C., Lorenzi, I., Rohrer, L. & von Eckardstein, A. Lipid efflux by the ATP-binding cassette transporters ABCA1 and ABCG1. *Biochim. Biophys. Acta* **1761**, 655–666 (2006).
19. Mulholland, C. V. et al. Propionate prevents loss of the PDIM virulence lipid in *Mycobacterium tuberculosis*. *Nat. Microbiol.* **9**, 1607–1618 (2024).
20. Quigley, J., et al. The cell wall lipid PDIM contributes to phagosomal escape and host cell exit of *Mycobacterium tuberculosis*. *mBio* **8**, e00148-17 (2017).
21. Alarcon, P. et al. Oleic and linoleic acids induce the release of neutrophil extracellular traps via pannexin 1-dependent ATP release and P2X1 receptor activation. *Front. Vet. Sci.* **7**, 260 (2020).
22. Jasenosky, L. D., Scriba, T. J., Hanekom, W. A. & Goldfeld, A. E. T cells and adaptive immunity to *Mycobacterium tuberculosis* in humans. *Immunol. Rev.* **264**, 74–87 (2015).
23. Kim, J. M., Rasmussen, J. P. & Rudensky, A. Y. Regulatory T cells prevent catastrophic autoimmunity throughout the lifespan of mice. *Nat. Immunol.* **8**, 191–197 (2007).
24. Simpson, T. R. et al. Fc-dependent depletion of tumor-infiltrating regulatory T cells co-defines the efficacy of anti-CTLA-4 therapy against melanoma. *J. Exp. Med.* **210**, 1695–1710 (2013).
25. Zhang, S. et al. Berbamine promotes macrophage autophagy to clear *Mycobacterium tuberculosis* by regulating the ROS/Ca^{2+} axis. *mBio* **14**, e0027223 (2023).
26. Pahari, S. et al. Induction of autophagy through CLEC4E in combination with TLR4: an innovative strategy to restrict the survival of *Mycobacterium tuberculosis*. *Autophagy* **16**, 1021–1043 (2020).
27. Silva, S. L. R. et al. Emetine induces oxidative stress, cell differentiation and NF-κB inhibition, suppressing AML stem/progenitor cells. *Cell Death Discov.* **10**, 201 (2024).
28. Dudhgaonkar, S. P., Tandan, S. K., Bhat, A. S., Jadhav, S. H. & Kumar, D. Synergistic anti-inflammatory interaction between meloxicam and aminoguanidine hydrochloride in carrageenan-induced acute inflammation in rats. *Life Sci.* **78**, 1044–1048 (2006).
29. Pellegrini, J. M. et al. Neutrophil autophagy during human active tuberculosis is modulated by SLAMF1. *Autophagy* **17**, 2629–2638 (2021).
30. Pizzimenti, S. et al. Oxidative stress-related mechanisms in melanoma and in the acquired resistance to targeted therapies. *Antioxidants* **10**, 1942 (2021).
31. Remans, P. H. et al. CTLA-4IG suppresses reactive oxygen species by preventing synovial adherent cell-induced inactivation of Rap1, a Ras family GTPASE mediator of oxidative stress in rheumatoid arthritis T cells. *Arthritis Rheum.* **54**, 3135–3143 (2006).
32. Gallegos, A. M., Pamer, E. G. & Glickman, M. S. Delayed protection by ESAT-6-specific effector $CD4^+$ T cells after airborne *M. tuberculosis* infection. *J. Exp. Med.* **205**, 2359–2368 (2008).
33. Linsley, P. S. & Golstein, P. Lymphocyte activation: T-cell regulation by CTLA-4. *Curr. Biol.* **6**, 398–400 (1996).
34. Trebak, M. & Kinet, J. P. Calcium signalling in T cells. *Nat. Rev. Immunol.* **19**, 154–169 (2019).
35. Prakriya, M. & Lewis, R. S. Store-operated calcium channels. *Physiol. Rev.* **95**, 1383–1436 (2015).
36. Patergnani, S. et al. Calcium signaling around mitochondria associated membranes (MAMs). *Cell Commun. Signal* **9**, 19 (2011).
37. Nava Lauson, C. B. et al. Linoleic acid potentiates $CD8^+$ T cell metabolic fitness and antitumor immunity. *Cell Metab.* **35**, 633–650 e639 (2023).
38. Tovey, S. C., Sun, Y. & Taylor, C. W. Rapid functional assays of intracellular Ca^{2+} channels. *Nat. Protoc.* **1**, 259–263 (2006).
39. Hobson, B. D. et al. Subcellular and regional localization of mRNA translation in midbrain dopamine neurons. *Cell Rep.* **38**, 110208 (2022).
40. Rule, C. S., Patrick, M. & Sandkvist, M. Measuring in vitro ATPase activity for enzymatic characterization. *J. Vis. Exp.* **114**, 54305 (2016).

41. Chandra, P., Grigsby, S. J. & Philips, J. A. Immune evasion and provocation by *Mycobacterium tuberculosis*. *Nat. Rev. Microbiol.* **20**, 750–766 (2022).
42. Sassetti, C. M. & Rubin, E. J. Genetic requirements for mycobacterial survival during infection. *Proc. Natl Acad. Sci. USA* **100**, 12989–12994 (2003).
43. Gupta, S. et al. Rv1273c, an ABC transporter of *Mycobacterium tuberculosis* promotes mycobacterial intracellular survival within macrophages via modulating the host cell immune response. *Int. J. Biol. Macromol.* **142**, 320–331 (2020).
44. Ambrozova, G., Pekarova, M. & Lojek, A. Effect of polyunsaturated fatty acids on the reactive oxygen and nitrogen species production by raw 264.7 macrophages. *Eur. J. Nutr.* **49**, 133–139 (2010).
45. Yan, B. et al. Linoleic acid metabolism activation in macrophages promotes the clearing of intracellular *Staphylococcus aureus*. *Chem. Sci.* **13**, 12445–12460 (2022).
46. Magdalon, J. et al. Oral administration of oleic or linoleic acids modulates the production of inflammatory mediators by rat macrophages. *Lipids* **47**, 803–812 (2012).
47. Jia, L. et al. *Porphyromonas gingivalis* aggravates colitis via a gut microbiota–linoleic acid metabolism–Th17/Treg cell balance axis. *Nat. Commun.* **15**, 1617 (2024).
48. Lin, L. et al. Oleic acid availability impacts thymocyte preprogramming and subsequent peripheral T_{reg} cell differentiation. *Nat. Immunol.* **25**, 54–65 (2024).
49. Guichard, V., et al. Calcium-mediated shaping of naive CD4 T-cell phenotype and function. *eLife* **6**, e27215 (2017).
50. Robert, C. A decade of immune-checkpoint inhibitors in cancer therapy. *Nat. Commun.* **11**, 3801 (2020).
51. Lazar-Molnar, E. et al. Programmed death-1 (PD-1)-deficient mice are extraordinarily sensitive to tuberculosis. *Proc. Natl Acad. Sci. USA* **107**, 13402–13407 (2010).
52. Tezera, L. B., et al. Anti-PD-1 immunotherapy leads to tuberculosis reactivation via dysregulation of TNF-alpha. *eLife* **9**, e52668 (2020).
53. Jayaraman, P. et al. TIM3 mediates T cell exhaustion during *Mycobacterium tuberculosis* infection. *PLoS Pathog.* **12**, e1005490 (2016).
54. Li, W. et al. MAGeCK enables robust identification of essential genes from genome-scale CRISPR/Cas9 knockout screens. *Genome Biol.* **15**, 554 (2014).
55. Abe, I. et al. Lipolysis-derived linoleic acid drives beige fat progenitor cell proliferation. *Dev. Cell* **57**, 2623–2637 e2628 (2022).
56. Rossi, A. M. & Taylor, C. W. Reliable measurement of free Ca^{2+} concentrations in the ER lumen using Mag-Fluo-4. *Cell Calcium* **87**, 102188 (2020).
57. Tekguc, M., Wing, J. B., Osaki, M., Long, J. & Sakaguchi, S. Treg-expressed CTLA-4 depletes CD80/CD86 by trogocytosis, releasing free PD-L1 on antigen-presenting cells. *Proc. Natl Acad. Sci. USA* **118**, e2023739118 (2021).

Acknowledgements

We thank B. Li (Shanghai Jiao-Tong University) for critical reading of the paper. We thank the members of the B.G. laboratory for discussions and technical assistance. This project was supported by grants from National Natural Science Foundation of China (32030038, 32188101, 918423003 and 31730025 to B.G.; 32394010 and 32394012 to Z.J., 82470001, 82270006, 82070007 to H.Y., 82122029, 82071776 to L.W.), the National Key R&D Program of China (2021YFA1300902 to H.Y.), Chinese National Program on Key Basic Research Project (2017YFA0505900 to B.G.), Science Project of Shanghai Municipal Health Commission (202040028 to Z.J.), the Fundamental Research Funds for the Central Universities (22120210624 and 22120240345 to Z.J.), CAMS Innovation Fund for Medical Sciences (2023-I2M-2-001 to Y.S.), and the Science and Technology Innovation Action Plan (STCSM, 24YF2735400 to H.C.).

Author contributions

H.C., S. Li, H.L., Z.J., Y.S., H.Y. and B.G. designed the study. S. Li, H.C. and H.L. performed most of the experiments and analysed the data. M.Y., J.W., X.H., S. Liu, Y.S. and H.Y. constructed the H37Rv genome-wide CRISPR KO mutant library. S. Li, H.Y., J.H., Y.Y., X.C. and J.X.W. constructed the H37Rv KO strain, performed metabolomics analysis and detected the level of linoleic acid. P.C., Y.C., R.Z., L.W., L.Q., C.G.F. and Q.Z. assisted with the preparation of the paper. S. Li, H.C., X.H., J.W., Z.L., Y.C. and Z.J. performed mouse infection experiments. The Mtb strains were stored by X.H. All authors discussed the results and commented on the paper.

Competing interests

The authors declare no competing interests.

Additional information

Extended data is available for this paper at https://doi.org/10.1038/s41564-025-02140-2.

Supplementary information The online version contains supplementary material available at https://doi.org/10.1038/s41564-025-02140-2.

Correspondence and requests for materials should be addressed to Yicheng Sun, Zhe Ji, Hua Yang or Baoxue Ge.

Peer review information *Nature Microbiology* thanks William Jacobs, Ye Zheng and the other, anonymous, reviewer(s) for their contribution to the peer review of this work.

Reprints and permissions information is available at www.nature.com/reprints.

Publisher's note Springer Nature remains neutral with regard to jurisdictional claims in published maps and institutional affiliations.

[1]Shanghai Key Laboratory of Tuberculosis, Shanghai Pulmonary Hospital, Tongji University School of Medicine, Shanghai, People's Republic of China. [2]Key Laboratory of Pathogen-Host Interaction, Ministry of Education, Department of Microbiology and Immunology, Tongji University School of Medicine, Shanghai, People's Republic of China. [3]NHC Key Laboratory of Systems Biology of Pathogens, State Key Laboratory of Respiratory Health and Multimorbidity, National Institute of Pathogen Biology and Center for Tuberculosis Research, Chinese Academy of Medical Sciences & Peking Union Medical College, Beijing, People's Republic of China. [4]Immunology and Host Defense Group, Faculty of Medicine and Health, The University of Sydney, Sydney, New South Wales, Australia. [5]Tuberculosis Research Program, Centenary Institute, The University of Sydney, Sydney, New South Wales, Australia. [6]Hongqiao International Institute of Medicine, Tongren Hospital & Shanghai Institute of Immunology, State Key Laboratory of Systems Medicine for Cancer, Shanghai Jiao Tong University School of Medicine, Shanghai, People's Republic of China. [7]Clinical Translation Research Center, Shanghai Pulmonary Hospital, Tongji University School of Medicine, Shanghai, People's Republic of China. [8]These authors contributed equally: Hongyu Cheng, Shenzhi Li, Hongjie Liu, Meiyi Yan, Jingxiang Wang. ✉e-mail: sunyc@ipbcams.ac.cnyang; jizhe@tongji.edu.cn; yanghua97065@tongji.edu.cn; gebaoxue@sibs.ac.cn

https://doi.org/10.1038/s41564-025-02140-2

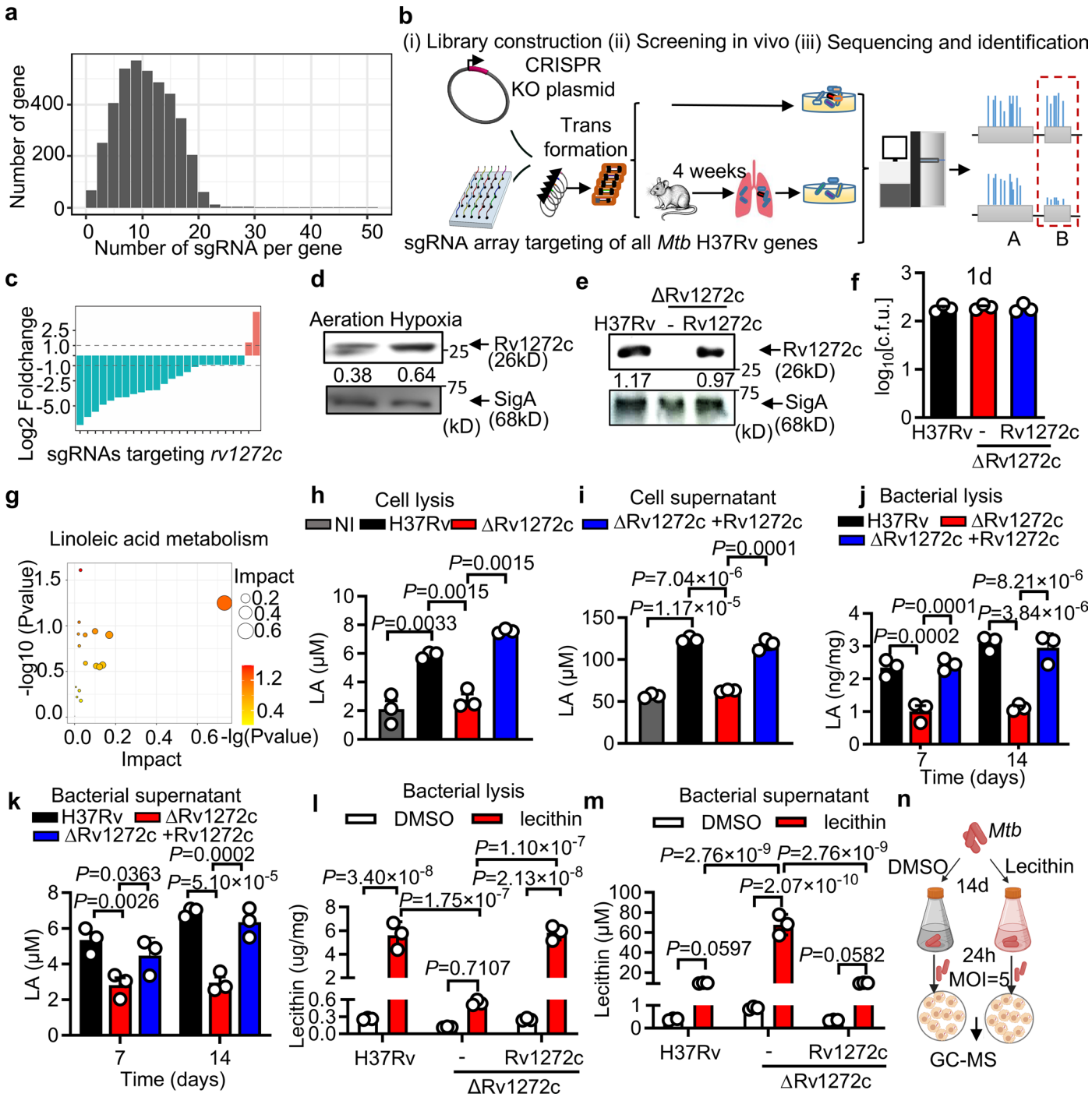

Extended Data Fig. 1 | Rv1272c induces linoleic acid export from Mtb-infected macrophages. (**a**) Distribution of designed sgRNAs in the Mtb H37Rv genome-wide clustered regularly interspaced short palindromic repeats (CRISPR) knockout (KO) mutant library. (**b**) C57BL/6 mice were infected with CRISPR KO library. At 4 weeks after infection, lung homogenates were plated on 7H10 agar to recover surviving bacteria. Genes required for survival in mice but not for growth in vitro were analyzed. (**c**) Variation of all mutants with sgRNAs targeting *rv1272c* were analyzed by comparing sgRNA abundance in infected mice to the original screening library. The dashed lines indicate the values of fold change that are equal to 2 and 0.5. The red and blue bars represent *Mtb* mutants with corresponding sgRNA that can and cannot survive in mice respectively. (**d**) Immunoblot (IB) of cell lysates from Mtb H37Rv incubated under aeration and hypoxia. Levels of Rv1272c and SigA proteins were quantified using ImageJ and grayscale ratio of Rv1272c/SigA were indicated below blots. (**e**) IB of cell lysates of indicated Mtb strains. Levels of Rv1272c and SigA proteins were quantified using ImageJ and grayscale ratio of Rv1272c/SigA were indicated below blots. (**f**) C57BL/6 mice were aerosol-infected with indicated Mtb strains (~200 c.f.u. per mouse). Bacterial loads in lung tissues at 1 day post infection were assayed by c.f.u. (**g**) Impact factor histogram showing metabolic pathways of metabolites in indicated Mtb-infected bone marrow-derived macrophages (BMDMs) culture supernatants. The enrichment significance was determined through hypergeometric testing with FDR correction. (**h, i**) Linoleic acid (LA) concentration in the cell lysis (**h**) or culture supernatants (**i**) of Mtb-infected BMDMs for 24 h. (**j, k**) Linoleic acid concentration in bacterial lysis (**j**) or culture supernatants (**k**) of Mtb incubated at normal condition for indicated days. (**l, m**) Assay of Lecithin concentration in lysis (**l**) or culture supernatants (**m**) of Mtb incubated with or without Lecithin (100 μM) for 14 days. (**n**) Schematic representation of experimental design for Fig. 1l, m. Data in **d-f, h-k, l, m** represent one experiment with three independent biological replicates ($n = 3$); mean ± s.e.m. Two-tailed unpaired Student's t-tests (**f, h, i**) and Two-way ANOVA with Tukey's multiple comparisons test (**j, k, l, m**) were used for statistical analyses.

https://doi.org/10.1038/s41564-025-02140-2

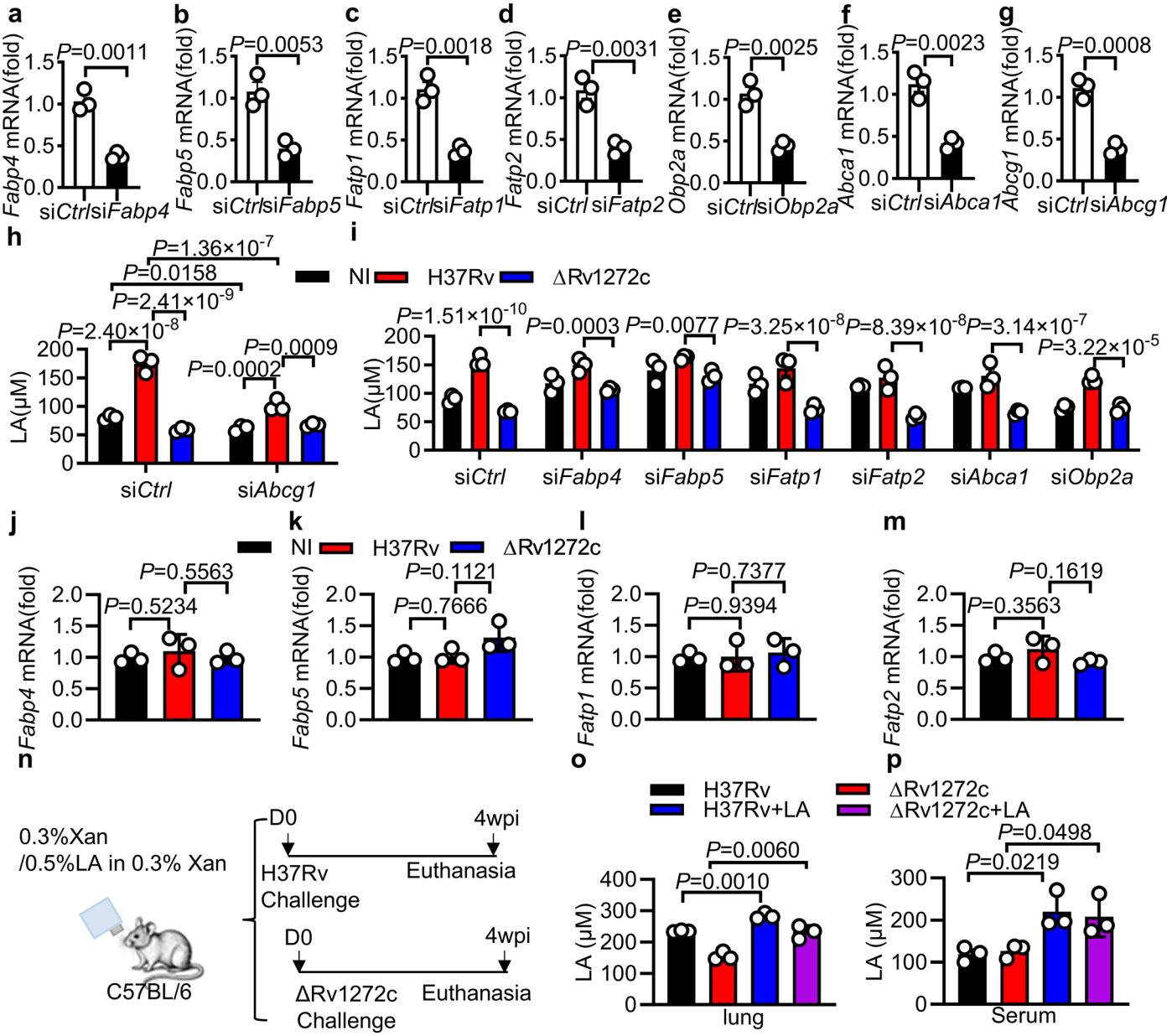

Extended Data Fig. 2 | Linoleic acid exports from Mtb-infected macrophages through ATP-binding cassette transporter G1 (ABCG1). (**a**-**g**) qPCR analysis of *Fabp4* (**a**), *Fabp5* (**b**), *Fatp1* (**c**), *Fatp2* (**d**), *Obp2a* (**e**), *Abca1* (**f**) and *Abcg1* (**g**) mRNA from BMDMs transfected with specific targeting siRNA or control siRNA. (**h**) Assay of linoleic acid concentration in the culture supernatants of Mtb-infected BMDMs transfected with *Abcg1* specific siRNA or control siRNA for 24 h. (**i**) Assay of linoleic acid concentration in the culture supernatants of Mtb-infected BMDMs transfected with specific siRNA targeting *Fabp4*, *Fabp5*, *Fatp1*, *Fatp2*, *Abca1*, *Obp2a*, or control siRNA for 24 h. (**j**-**m**) qPCR analysis of *Fabp4* (**j**), *Fabp5* (**k**), *Fatp1* (**l**) and *Fatp2* (**m**) mRNA from BMDMs infected with Mtb H37Rv or H37RvΔRv1272c strains for 24 h. (**n**) Schematic representation of mice experimental design for Fig. 1n–p. C57BL/6 mice were aerosol-infected with approximately 200 c.f.u. per mouse of indicated Mtb strains and treated with or without linoleic acid. (**o**, **p**) C57BL/6 mice were aerosol-infected with approximately 200 c.f.u. per mouse of indicated Mtb strains and treated with or without linoleic acid. Linoleic acid concentrations in lung homogenate supernatants (**o**) and serum (**p**) were analyzed at 4 weeks post infection. Data in **a**-**m**, **o**, **p** represent one experiment with three independent biological replicates ($n = 3$); mean ± s.e.m. Two-tailed unpaired Student's t-tests (**a**-**g**, **j**-**m**, **o**, **p**) and Two-way ANOVA with Tukey's multiple comparisons test (**h**, **i**) were used for statistical analyses.

https://doi.org/10.1038/s41564-025-02140-2

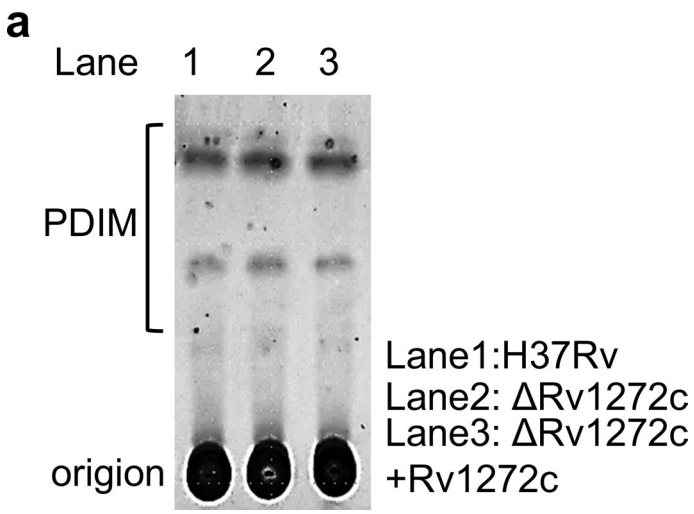

Extended Data Fig. 3 | TLC analysis of phthiocerol dimycocerosate (PDIM) production in Mtb strains. TLC analysis of PDIM production by Mtb H37Rv, H37RvΔRv1272c and H37Rv(ΔRv1272c + Rv1272c) strains. Three hundred micrograms of total lipid was loaded in each lane. The plate was resolved in a mobile phase of 9:1 petroleum ether-diethyl ether. Lipid spots were revealed by charring. Data of **a** represents one experiment with three independent biological replicates ($n = 3$).

https://doi.org/10.1038/s41564-025-02140-2

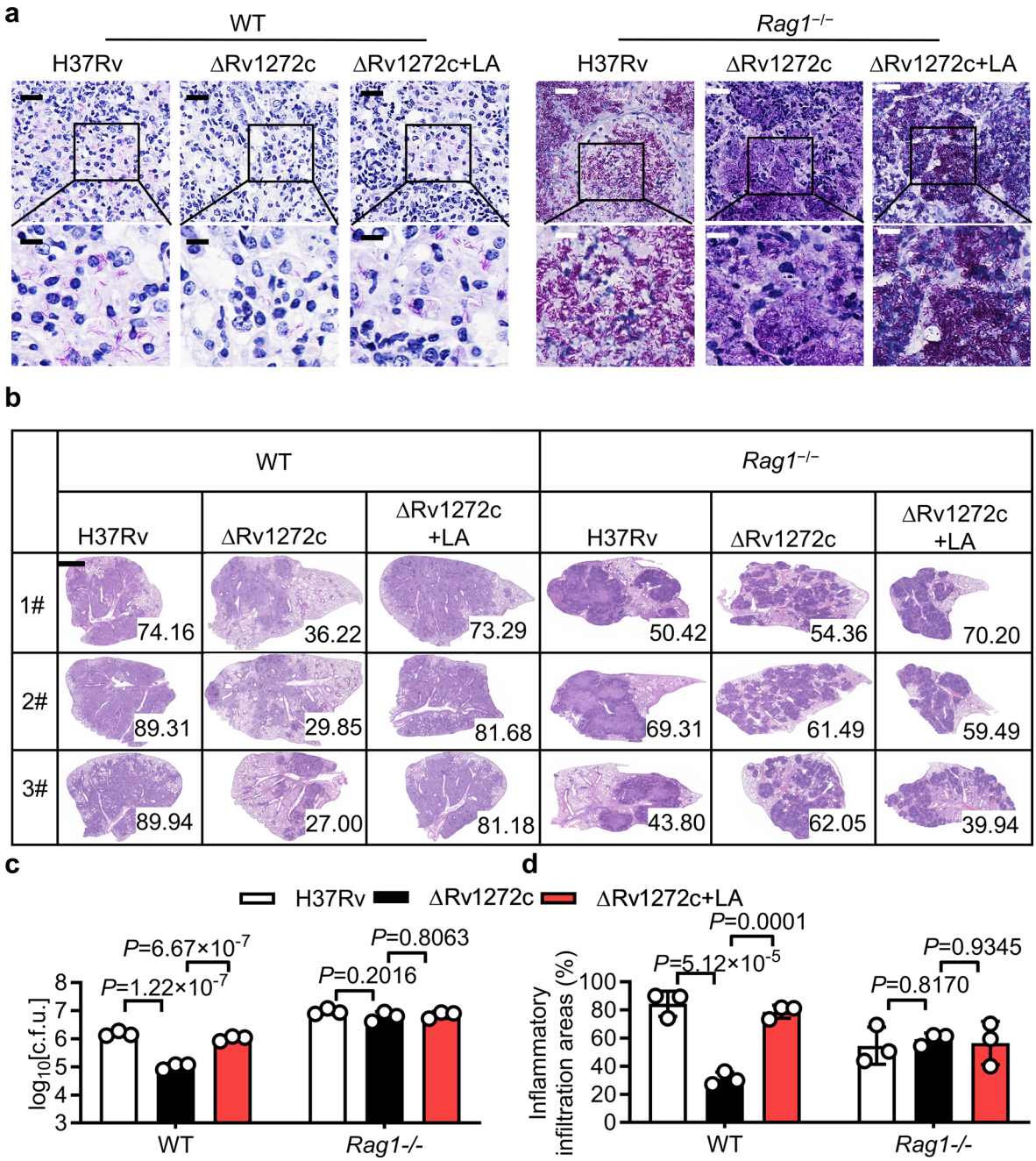

Extended Data Fig. 4 | Rv1272c or linoleic acid promotes Mtb survival in vivo via inhibiting adaptive immunity. (**a-d**) WT mice and *Rag1*$^{-/-}$ mice were aerosol-infected with ~200 c.f.u. per mouse of indicated Mtb strains and treated with or without linoleic acid. After 4 weeks of infection, histopathology of lung sections from infected mice was assessed via acid-fast staining (**a**; scale bar = 100 μm [upper] and 20 μm [lower]), H&E staining (scale bar=1 mm) (**b**), bacterial c.f.u. (**c**) and quantified inflammatory areas (**d**). #1–3 indicate three representative lung sections. Quantified inflammatory areas are shown in sections. Data in **a-d** represent one experiment with three independent biological replicates ($n = 3$); mean ± s.e.m. Two-way ANOVA with Tukey's multiple comparisons test (**c, d**) were used for statistical analyses.

https://doi.org/10.1038/s41564-025-02140-2

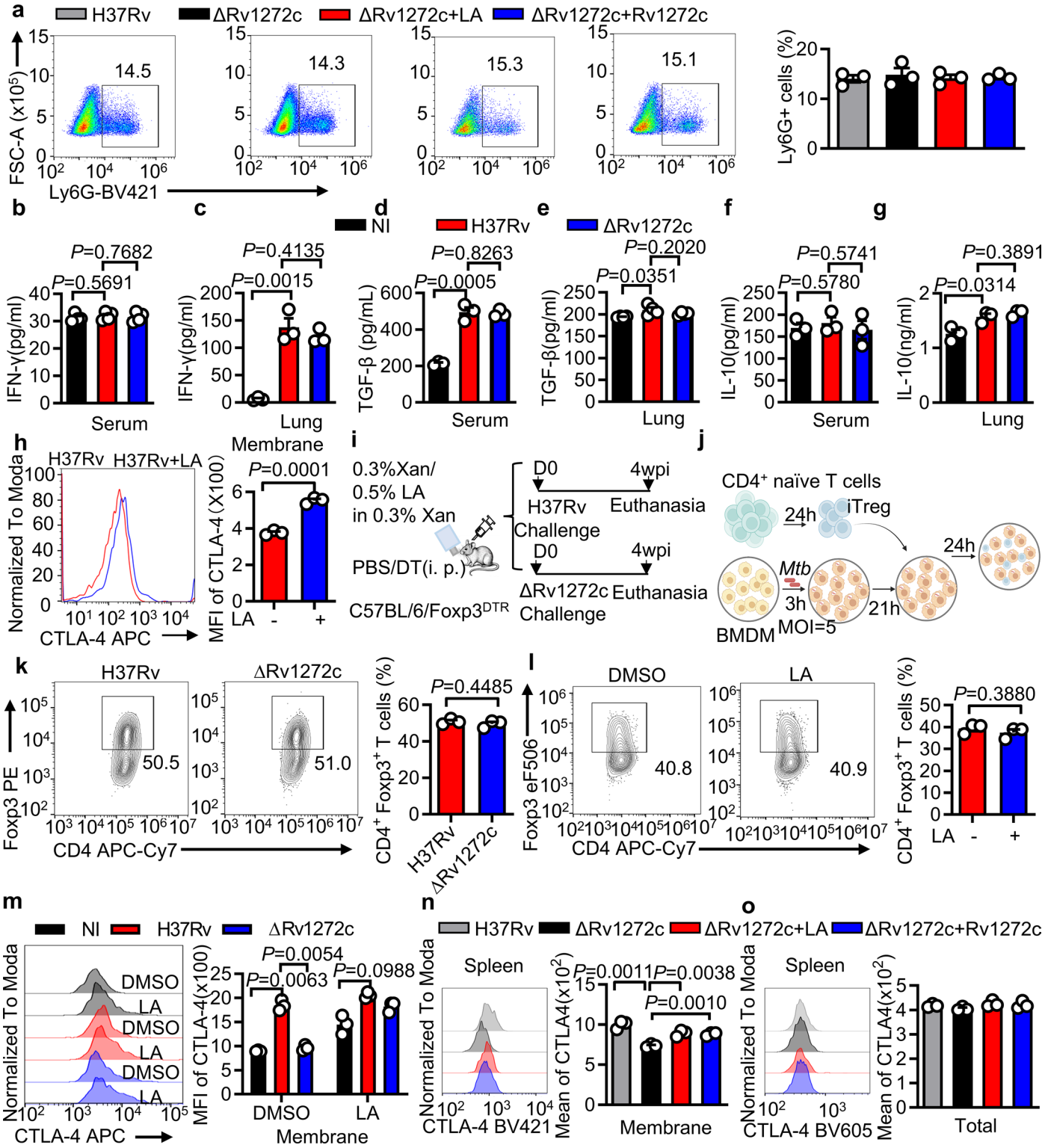

Extended Data Fig. 5 | See next page for caption.

https://doi.org/10.1038/s41564-025-02140-2

Extended Data Fig. 5 | Rv1272c or linoleic acid promotes the intramacrophage survival of Mtb via Treg cells. (**a**) C57BL/6 mice were aerosol-infected with approximately 200 c.f.u. per mouse of indicated Mtb strains. Percentages of $CD45^+Ly6G^+$ cells were measured using FCM. (**b**-**g**) C57BL/6 mice were aerosol-infected with approximately 200 c.f.u. per mouse of indicated Mtb strains. IFN-γ, TGF-β and IL-10 concentrations in serum (**b**, **d**, **f**) and lung homogenate supernatants (**c**, **e**, **g**) were analyzed at 4 weeks post infection. (**h**) C57BL/6 mice were aerosol-infected with approximately 200 c.f.u. per mouse of Mtb H37Rv and administered with linoleic acid for 4 weeks. Mean Fluorescence Intensity (MFI) of membrane CTLA-4 levels were measured in $CD4^+$ Tregs in lung tissues. (**i**) Schematic representation of mice experimental design for Fig. 2j, k. (**j**) Schematic representation of Mtb-infected BMDMs and $CD4^+$ Tregs co-culture experimental design for Fig. 2m, n. (**k**) After 1 day of infection with Mtb strains, BMDMs were co-incubated with $CD4^+$ Treg cells for 1 day, and percentage of $Foxp3^+CD4^+$ T cells was measured in $CD4^+$ T cells. (**l**) After 1 day of infection with Mtb H37Rv strains, BMDMs were co-incubated with $CD4^+$ Treg cells treated with or without linoleic acid for 24 h, percentage of $Foxp3^+CD4^+$ T cells was measured in $CD4^+$ T cells. (**m**) After 1 day of infection with indicated Mtb strains (MOI = 5), BMDMs were co-incubated with $CD4^+$ Treg cells treated with or without linoleic acid for 1 day, MFI of membrane CTLA-4 levels in $CD4^+$ Tregs were measured by FCM. (**n**, **o**) C57BL/6 mice were aerosol-infected with approximately 200 c.f.u. per mouse of *Mtb* H37Rv and administered with linoleic acid for 4 weeks. MFI of membrane (**n**) and total (**o**) CTLA-4 levels were measured in $CD4^+$ Tregs in spleen tissues. Data in **a**-**h**, **k**-**o** represent one experiment with at least three independent biological replicates (**a**,**c**-**d**,**f**-**h**,**k**-**o**, $n = 3$; **b**,**e**, $n = 4$); mean ± s.e.m. Two-tailed unpaired Student's t-tests (**a**-**h**, **k**, **l**, **n**, **o**) and Two-way ANOVA with Tukey's multiple comparisons test (**m**) were used for statistical analyses. Panel **j** created with BioRender.com.

https://doi.org/10.1038/s41564-025-02140-2

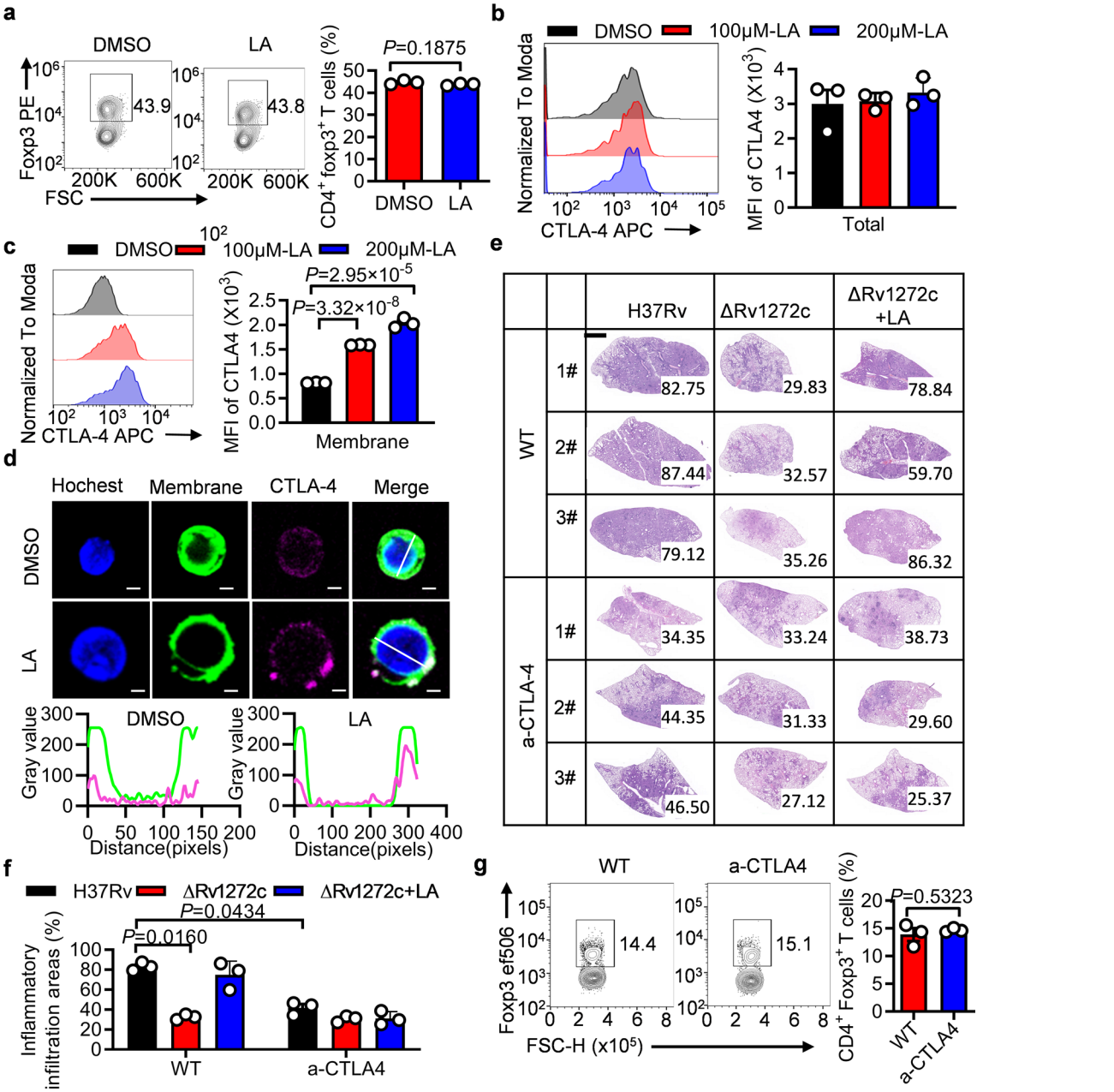

Extended Data Fig. 6 | Linoleic acid promotes mycobacteria survival via CTLA-4 of Tregs in vivo. (**a**) Naïve $CD4^+$ T cells were stimulated with anti-CD3 and anti-CD28 antibodies in the presence of IL-2 and TGF-β for 3 days and treated with or without linoleic acid (100 μM). The percentage of $Foxp3^+CD4^+$ T cells was measured in $CD4^+$ T cells. (**b**-**d**) Naïve $CD4^+$ T cells were stimulated with anti-CD3 and anti-CD28 antibodies in the presence of IL-2 and TGF-β for 3 days and treated with or without linoleic acid (100 μM or 200 μM). MFI of total (**b**) and membrane (**c**) CTLA-4 levels of $CD4^+$ Tregs were measured by FCM. (**d**) Immunofluorescence data shows Hoechst (Blue), membrane (Green), and CTLA-4 (Magenta) staining in $CD4^+$ Tregs. Below, pixel intensity plot for dashed line; Scale bar = 1 μm. (**e**-**g**) C57BL/6 mice treated with/without anti-CTLA-4 antibodies (500 μg/mouse) on 4, 8, 12, 16, 20, and 24 days post-infection were aerosol-infected with approximately 200 c.f.u. per mouse of indicated Mtb strains and treated with or without linoleic acid via drinking water. After 4 weeks of infection, histopathology (scale bar=1 mm) of lung sections was assessed via H&E staining. #1–3 indicate three representative lung sections (**e**). Quantified inflammatory areas in the lung tissues of mice infected with Mtb strains were analyzed at 4 weeks post infection (**f**). The percentage of $Foxp3^+CD4^+$ T cells was measured in $CD4^+$ T cells (**g**). Data in **a**-**g** represent one experiment with three independent biological replicates ($n = 3$); mean ± s.e.m. Two-tailed unpaired Student's t-tests (**a**-**c**, **g**) and Two-way ANOVA with Tukey's multiple comparisons test (**f**) were used for statistical analyses.

https://doi.org/10.1038/s41564-025-02140-2

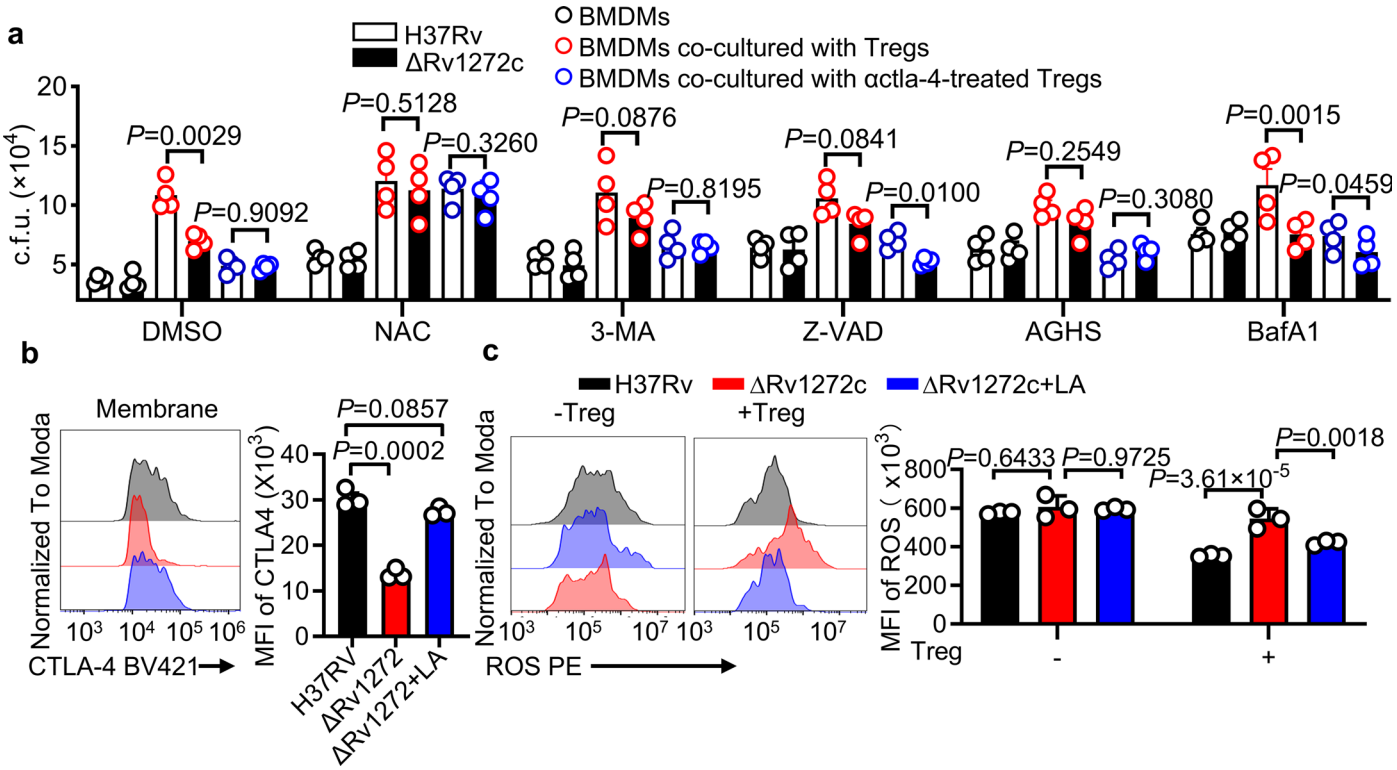

Extended Data Fig. 7 | Rv1272c induced linoleic acid promotes CTLA-4 surface trafficking on Tregs to inhibit cytosol ROS and facilitate the survival of Mtb in macrophages. (**a**) Mtb-infected BMDMs (MOI = 5) were pretreated with indicated inhibitors for 24 h and then co-cultured with Tregs treated with isotype control IgG or anti-CTLA-4 blocking antibody (40 μg/mL) for 1 day, intracellular survival of the indicated Mtb strains in BMDMs infected for 2 days were determined using c.f.u. assay. (**b**) After 1 day of infection with indicated Mtb strains (MOI = 5), BMDMs were co-incubated with $CD4^+$ ESAT6-specific Treg cells treated with or without linoleic acid for 24 h, MFI of membrane CTLA-4 levels in $CD4^+$ Tregs were measured by FCM. (**c**) After 1 day of infection with indicated Mtb strains (MOI = 5), BMDMs were co-incubated with $CD4^+$ ESAT6-specific Treg cells treated with or without linoleic acid for 24 h. MFI of ROS levels in BMDMs were measured by FCM. Data in a-e represent one experiment with at least three independent biological replicates (**a**, $n = 4$; **b**-**c**, $n = 3$); mean ± s.e.m. Two-tailed unpaired Student's t-tests (**b**) and Two-way ANOVA with Tukey's multiple comparisons test (**a**, **c**) were used for statistical analyses.

https://doi.org/10.1038/s41564-025-02140-2

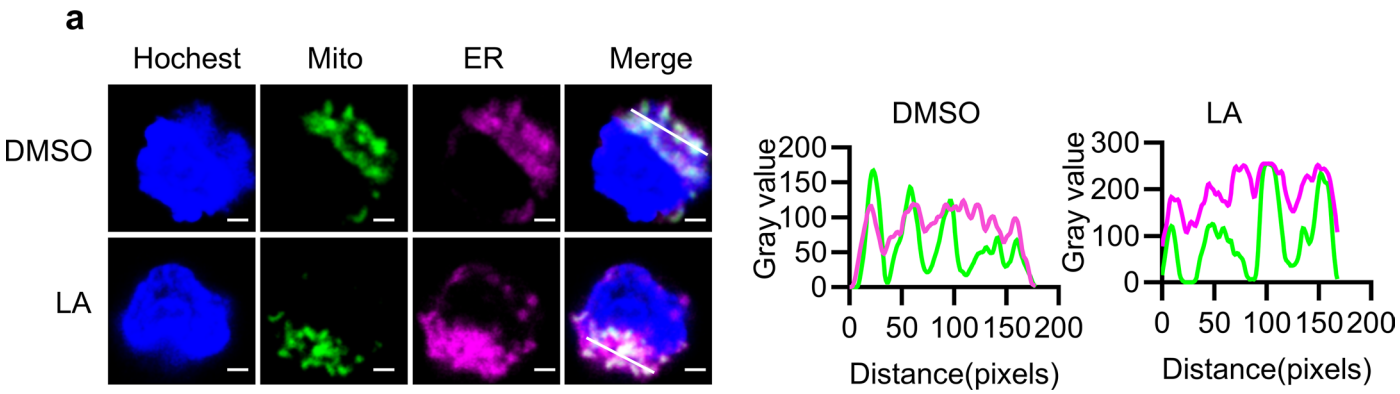

Extended Data Fig. 8 | Linoleic acid promotes the formation of mitochondria-associated ER membranes (MAMs). Naïve $CD4^+$ T cells were stimulated with anti-CD3 and anti-CD28 antibodies in the presence of IL-2 and TGF-β for 3 days and treated with or without linoleic acid (100 μM). Immunofluorescence data shows Hoechst (Blue), Mito-Traker (Green), and ER-Traker (Magenta) staining in $CD4^+$ Tregs. Right, pixel intensity plot for dashed line. Scale bar = 1 μm. Data of **a** represents one experiment with three independent biological replicates ($n = 3$).

https://doi.org/10.1038/s41564-025-02140-2

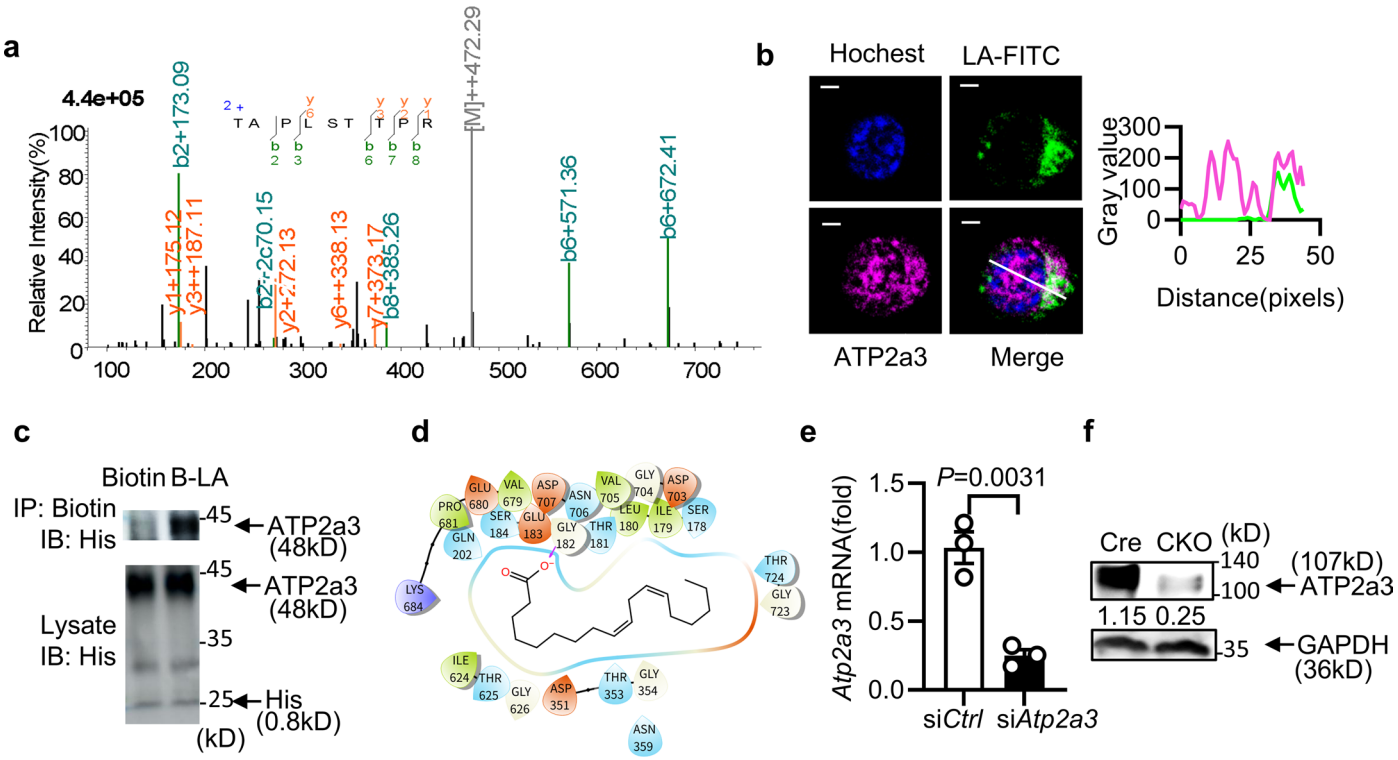

Extended Data Fig. 9 | Linoleic acid interacts with ATP2a3. (**a**) Representative mass spectrum of interacting proteins for linoleic acid identified by Liquid Chromatography Mass Spectrometry (LC-MS)/MS analysis. (**b**) Naïve $CD4^+$ T cells were stimulated with anti-CD3 and anti-CD28 antibodies in the presence of IL-2 and TGF-β for 3 days and treated with DMSO or FITC-linoleic acid (100 μM). Immunofluorescence data shows Hoechst (Blue), linoleic acid-FITC (Green), and ATP2a3 (Magenta) staining in $CD4^+$ Tregs. Scale bar = 1 μm. (**c**) Direct interaction of linoleic acid with ATP2a3 was detected using pull-down assay in vitro. (**d**) Predicted potential binding sites between linoleic acid and ATP2a3 using AlphaFold. (**e**) qPCR analysis of *Atp2a3* mRNA from $CD4^+$ Tregs transfected with *Atp2a3* specific siRNA or control siRNA. (**f**) The ATP2a3 protein levels of splenic $CD4^+Foxp3^+$ Treg cells isolated from $Foxp3^{cre}$ (Cre) and $Foxp3^{cre}Atp2a3^{fl/+}$ (CKO) mice. Data in **b, c, e, f** represent one experiment with three independent biological replicates ($n = 3$); mean ± s.e.m. Two-tailed unpaired Student's t-tests (**e**) was used for statistical analyses.

https://doi.org/10.1038/s41564-025-02140-2

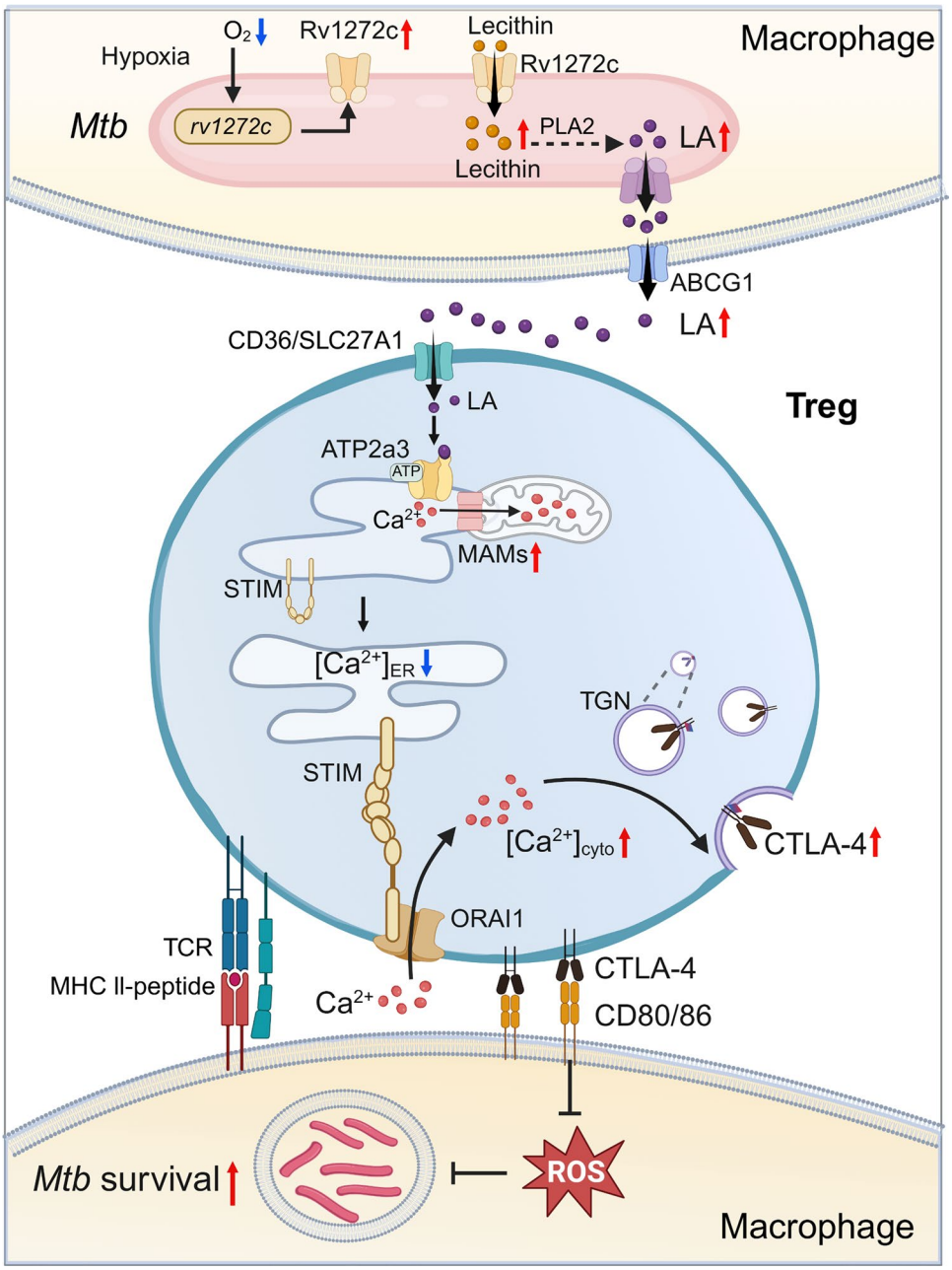

Extended Data Fig. 10 | Summary diagram. Hypoxia-induced *Mtb* Rv1272c enhanced the import of lecithin, leading to the generation of linoleic acid (LA) and subsequent release of LA from *Mtb*-infected macrophages through ATP Binding Cassette Subfamily G Member 1 (ABCG1). The released LA directly interacted with ATP2a3 and enhanced the formation of MAMs, which facilitated Ca^{2+} transfer from ER to mitochondria via the mitochondrial calcium uniporter (MCU), leading to ER Ca^{2+} depletion in Tregs. Reduced ER Ca^{2+} subsequently triggered store-operated calcium entry (SOCE), thus elevating cytosolic Ca^{2+} levels and Ca^{2+}-dependent CTLA-4 surface trafficking, which reduced ROS levels in macrophages and promoted mycobacterial intracellular survival. Figure created with BioRender.com.

nature portfolio

Corresponding author(s): Yicheng Sun, Zhe Ji, Hua Yang and Baoxue Ge

Last updated by author(s): Aug 22, 2025

Reporting Summary

Nature Portfolio wishes to improve the reproducibility of the work that we publish. This form provides structure for consistency and transparency in reporting. For further information on Nature Portfolio policies, see our Editorial Policies and the Editorial Policy Checklist.

Statistics

For all statistical analyses, confirm that the following items are present in the figure legend, table legend, main text, or Methods section.

n/a	Confirmed	
☐	☒	The exact sample size (*n*) for each experimental group/condition, given as a discrete number and unit of measurement
☐	☒	A statement on whether measurements were taken from distinct samples or whether the same sample was measured repeatedly
☐	☒	The statistical test(s) used AND whether they are one- or two-sided *Only common tests should be described solely by name; describe more complex techniques in the Methods section.*
☒	☐	A description of all covariates tested
☒	☐	A description of any assumptions or corrections, such as tests of normality and adjustment for multiple comparisons
☐	☒	A full description of the statistical parameters including central tendency (e.g. means) or other basic estimates (e.g. regression coefficient) AND variation (e.g. standard deviation) or associated estimates of uncertainty (e.g. confidence intervals)
☐	☒	For null hypothesis testing, the test statistic (e.g. *F*, *t*, *r*) with confidence intervals, effect sizes, degrees of freedom and *P* value noted *Give P values as exact values whenever suitable.*
☒	☐	For Bayesian analysis, information on the choice of priors and Markov chain Monte Carlo settings
☒	☐	For hierarchical and complex designs, identification of the appropriate level for tests and full reporting of outcomes
☒	☐	Estimates of effect sizes (e.g. Cohen's *d*, Pearson's *r*), indicating how they were calculated

Our web collection on statistics for biologists contains articles on many of the points above.

Software and code

Policy information about availability of computer code

Data collection	The CRISPR KO library sequencing data collection was performed with NovaSeq 6000 system (Illumina, USA). The western blot data collection was performed with ImageQuant LAS 4000mini and Amersham Imager 600. Confocol data was obtained with Leica SP8 microscope. The flow cytometry data was obtained using BD FACSDiva and cytoflex cytexpert. Analyses were carried out using a LECO Pegasus® instrument (LECO, St. Joseph, MI,USA) consisting of an Agilent 8890A GC (Agilent Technologies, Palo Alto, CA, USA) system (Metabolomics analysis). GC-MS analysis was performed using an Agilent 7890B gas chromatograph system coupled with a Agilent 5977B mass spectrometer(LA assays). Ultra-high performance liquid chromatography-MS/MS (UHPLC-MS/MS) carried out using an Agilent 1290 Infinity II series UHPLC System (Agilent Technologies), equipped with a Waters Waters ACQUITY UPLC BEH C18 (150 * 2.1 mm, 1.7 µm, Waters) for UHPLC, and an Agilent 6460 triple quadrupole mass spectrometer (Agilent Technologies), equipped with an AJS electrospray ionization (AJS-ESI) interface, was applied for MS assay(Lecithin assays). The SPR data was detected by OpenSPRTM (Nicoya Lifesciences, Waterloo, Canada). ELISA assay data was obtained with Tecan NanoQuant Infinite M200 PRO. And, qPCR data was obtained using LC480 thermocycler (Roche, Indianapolis, IN, USA).
Data analysis	Alignment to the library and the count of the sgRNAs were performed using MAGeCK(v0.5.7). Data analysis of flow cytometry was performed with FlowJo 10. Hematoxylin and eosin or Ziehl–Neelsen (for acid-fast bacilli) stains image data was obtained using an automated whole-slide scanning device (3DHISTECH, Sysmex). Data analysis of ELISA was performed with i-control™(2.0). Date analysis of western blot and conforcal were quantified using ImageJ. Statistical analysis of data was obtained using Prism Graphpad 9.0.

For manuscripts utilizing custom algorithms or software that are central to the research but not yet described in published literature, software must be made available to editors and reviewers. We strongly encourage code deposition in a community repository (e.g. GitHub). See the Nature Portfolio guidelines for submitting code & software for further information.

Data

Policy information about availability of data

All manuscripts must include a data availability statement. This statement should provide the following information, where applicable:

- Accession codes, unique identifiers, or web links for publicly available datasets
- A description of any restrictions on data availability
- For clinical datasets or third party data, please ensure that the statement adheres to our policy

The metabolomics datasets for the analysis of Mtb-infected BMDM culture supernatant profiles are available in the MetaboLights database under accession number MTBLS12875. The CRISPR KO screening analysis data and the mass spectrometry data for comparative metabolomics analysis are provided as Supplementary Tables 1–2. The other primary source data are provided within this paper. Original western blot and TLC images are provided as Source data.

Research involving human participants, their data, or biological material

Policy information about studies with human participants or human data. See also policy information about sex, gender (identity/presentation), and sexual orientation and race, ethnicity and racism.

Reporting on sex and gender	not applicable
Reporting on race, ethnicity, or other socially relevant groupings	not applicable
Population characteristics	not applicable
Recruitment	not applicable
Ethics oversight	not applicable

Note that full information on the approval of the study protocol must also be provided in the manuscript.

Field-specific reporting

Please select the one below that is the best fit for your research. If you are not sure, read the appropriate sections before making your selection.

☒ Life sciences ☐ Behavioural & social sciences ☐ Ecological, evolutionary & environmental sciences

For a reference copy of the document with all sections, see nature.com/documents/nr-reporting-summary-flat.pdf

Life sciences study design

All studies must disclose on these points even when the disclosure is negative.

Sample size	No statistical methods were used to pre-determine sample sizes, but our sample sizes are similar to those reported in previous publications
Data exclusions	No data were excluded from analysis.
Replication	We have indicated the number of independent experiments performed in the figure legends or the method.
Randomization	Data collection was randomized and animals/samples were assigned to the various experimental groups randomly.
Blinding	The data collection and analysis were not performed blind to the conditions of the experiments.

Reporting for specific materials, systems and methods

We require information from authors about some types of materials, experimental systems and methods used in many studies. Here, indicate whether each material, system or method listed is relevant to your study. If you are not sure if a list item applies to your research, read the appropriate section before selecting a response.

Materials & experimental systems

n/a	Involved in the study
☐	☒ Antibodies
☒	☐ Eukaryotic cell lines
☒	☐ Palaeontology and archaeology
☐	☒ Animals and other organisms
☒	☐ Clinical data
☒	☐ Dual use research of concern
☒	☐ Plants

Methods

n/a	Involved in the study
☒	☐ ChIP-seq
☐	☒ Flow cytometry
☒	☐ MRI-based neuroimaging

Antibodies

Antibodies used

WB or immunoprecipitation (IP) (dilutions are shown for WB and IP experiments): anti-SigA (BioLegend, 663205; 1:1000), anti-Rv1272c (Gene Optimal, 1:1000), anti-GAPDH (Sigma, G9545; 1:5000), anti-β-actin (Sigma, A5441; 1:5000), goat anti-Rabbit IgG antibody, Peroxidase Conjugated (Sigma, AP132P; 1:5000), HRP-conjugated Goat anti-Mouse IgG (H+L) (ABclonal, AS003; 1:5000), anti-SERCA3 monoclonal antibody (Proteintech Group, 1A2C2; 1:1000).
Immunostaining reagents: Rabbit polyclonal anti-ATP2a3 (Affinity Biosciences, DF15345; 1:200), goat anti-rabbit IgG (H+L) cross-adsorbed secondary antibody, Alexa Fluor 568 (Thermo Fisher, A-11011; 1:1000), Armenian Hamster monoclonal CTLA-4 antibody (1B8) [DyLight 594] (Novus, NBP1-41000DL594).
Flow cytometry (FCM) reagents: Anti-CD45 antibody (eBioscience, 30F11; 1:200), anti-CD3e (eBioscience, 145-2C11; 1:200), anti-CD4 (Biolegend, GK1.5; 1:200), anti-T-bet (Invitrogen, 4B10; 1:100), anti-CD25 (Invitrogen, PC61.5; 1:200), anti-CD8a (Invitrogen, 53-6.7; 1:200), anti-FOXP3 (Invitrogen, FJK-16S; 1:100), anti-CD152 (Biolegend, UC10-4B9; 1:200), I-Ab ESAT-61-20 Tetramer-PE (MBL, TS-M707-1; 1:50), anti-Ly-6G (BD Biosciences, 562737; 1:200).

Validation

The commercial antibodies are well used and reported in lots of previous publications. Antibodies against Rv1272c were generated by immunizing BALB/c mice with a recombinant protein antigen of Rv1272c.
Validation statement for anti-GAPDH https://www.sigmaaldrich.cn/CN/zh/product/sigma/g9545
Validation statement for Goat Anti-Rabbit IgG Antibody, Peroxidase Conjugated https://www.merckmillipore.com/CN/zh/product/Goat-Anti-Rabbit-IgG-Antibody-Peroxidase-Conjugated,MM NF-AP132P
Validation statement for HRP-conjugated Goat anti-Mouse IgG (H+L) https://static.abclonal.com/datasheet/AS003.pdf
Validation statement for Rabbit polyclonal anti-ATP2a3 https://www.affbiotech.com/goods-19789-DF15345-ATP2A3_Antibody.html
Validation statement for SERCA3 Monoclonal antibody https://www.ptgcn.com/products/SERCA3-Antibody-68287-1-Ig.htm
Validation statement for anti-SigA https://www.biolegend.com/en-us/products/direct-blot-hrp-anti-eme-coli-em-rna-sigma-70-antibody-13486
Validation statement for goat anti-rabbit IgG (H+L) cross-adsorbed secondary antibody, Alexa Fluor 568 https://www.thermofisher.cn/cn/zh/antibody/product/Goat-anti-Rabbit-IgG-H-L-Cross-Adsorbed-Secondary-Antibody-Polyclonal/A-11011
Validation statement for anti-CD3e https://www.thermofisher.cn/antibody/primary/query/145-2C11
Validation statement for anti-CD4 https://www.biolegend.com/en-us/products/apc-cyanine7-anti-mouse-cd4-antibody-1964
Validation statement for anti-T-bet https://www.thermofisher.cn/cn/zh/antibody/product/T-bet-Antibody-clone-eBio4B10-4B10-Monoclonal/50-5825-82
Validation statement for anti-CD25 https://www.thermofisher.cn/cn/zh/antibody/product/CD25-Antibody-clone-PC61-5-Monoclonal/25-0251-82
Validation statement for anti-CD8a https://www.thermofisher.cn/cn/zh/antibody/product/CD8a-Antibody-clone-53-6-7-Monoclonal/45-0081-82
Validation statement for anti-FOXP3 https://www.thermofisher.cn/cn/zh/antibody/product/FOXP3-Antibody-clone-FJK-16s-Monoclonal/12-5773-82
Validation statement for anti-CD152 https://www.biolegend.com/en-gb/products/apc-anti-mouse-cd152-antibody-5455
Validation statement for anti-Ly-6G https://www.bdbiosciences.com/zh-cn/products/reagents/flow-cytometry-reagents/research-reagents/single-color-antibodies-ruo/bv605-rat-anti-mouse-ly-6g.563005?tab=product_details
Validation statement for anti-CD45 https://www.thermofisher.cn/cn/zh/antibody/product/CD45-Antibody-clone-30-F11-Monoclonal/11-0451-82

Animals and other research organisms

Policy information about studies involving animals; ARRIVE guidelines recommended for reporting animal research, and Sex and Gender in Research

Laboratory animals

All animal experiments were approved by the Animal Experiment Administration Committee of Tongji University School of Medicine (TJAA06520101) and followed the National Institutes of Health (NIH) Guidelines for the Care and Use of Laboratory Animals. B6. Cg-Thy1a Tg (CD2-Tcra,-Tcrb) 27Glkm/J (C7 TCR tg.CD90.1) mice (Strain #:035728; RRID:IMSR_JAX:035728) express a T cell receptor specific for the immunodominant Mtb antigen ESAT-6 (early secreted antigenic target 6) from the human CD2 T cell promoter was

	purchased from The Jackson Laboratory. Ctla4-floxed mice, Atp2a3-floxed mice, Foxp3Cre mice and Rag1−/− mice were purchased from Cyagen. Foxp3CreERT2 transgenic mice were provided by Prof Qiang Zou (Shanghai Jiao-Tong University, China). The Ctla4-floxed mice were crossed with Foxp3CreERT2 transgenic mice to produce age-matched Ctla4fl/+Foxp3CreERT2 mice. The Atp2a3-floxed mice were crossed with Foxp3Cre transgenic mice to produce age-matched Atp2a3fl/+Foxp3Cre mice. Foxp3DTR mice were purchased from Cyagen Biosciences Inc. and Shanghai Model Organisms Center, Inc. (NM-KI-190046). Genetic models were on a C57BL/6 background. All mice were bred in specific pathogen-free conditions at the Shanghai Pulmonary Hospital Laboratory Animal Center (temperature between 20 and 26 °C, relative humidity between 50% and 60%, light intensity in the feeding room 15–20 lx with 12 h:12 h light: dark cycle) and fed with 25 kGy irradiated feed (SLAC, P1101F) in accordance with hospital guidelines.
Wild animals	The study did not involve wild animals.
Reporting on sex	All mice were age-, weight, and sex-matched in each experiment.
Field-collected samples	The study did not involve samples collected from the field.
Ethics oversight	All animal experiments were reviewed and approved by the Animal Experiment Administration Committee of our university and were conducted in accordance with the National Institutes of Health (NIH) Guidelines for the Care and Use of Laboratory Animals.

Note that full information on the approval of the study protocol must also be provided in the manuscript.

Plants

Seed stocks	not applicable
Novel plant genotypes	not applicable
Authentication	not applicable

Flow Cytometry

Plots

Confirm that:

☒ The axis labels state the marker and fluorochrome used (e.g. CD4-FITC).

☒ The axis scales are clearly visible. Include numbers along axes only for bottom left plot of group (a 'group' is an analysis of identical markers).

☒ All plots are contour plots with outliers or pseudocolor plots.

☒ A numerical value for number of cells or percentage (with statistics) is provided.

Methodology

Sample preparation	For surface marker analyses, cells were incubated in PBS plus bovine serum albumin (2%, w/v) (Sigma) for 30 min on ice. In phospho-FC analyses, and to preserve fluorescent proteins, cells were fixed in paraformaldehyde (2%) at room temperature for 30 min, permeabilization in ice-cold methanol (90%) for 30 min, and then incubated at room temperature in 1 × permeabilization buffer (eBioscience, 00-8333-56) for 30 min. For transcription factor staining, FOXP3/transcription factor staining buffers were used (eBioscience, 00-5523-00). For intracellular cytokine staining, a fixation/permeabilization kit was used (BD Biosciences, 554714). Cells for intracellular cytokine staining were activated using a cell stimulation cocktail (eBioscience, 00-4975-93). Cells were stained with surface markers, fixed, and permeabilized using a fixation/ permeabilization kit (BD Biosciences), and stained with anti-IFN-γ (Biolegend, XMG1.2) and anti-IL-10 antibodies (Invitrogen, JES5-16E3). Cells were washed twice and IFN-γ+ CD8+T frequencies determined by FC. Mitochondrial mass (Thermo Fisher, M7514) and ROS levels (Beyotime, S0033S) were determined by FC. Mitochondrial ROS (Thermo Fisher, M36008) was also determined using FC. Fluorescence minus one controls were acquired to discriminate between positive versus negative signals for CTLA-4 and ROS stains.
Instrument	CytoFLEX LX and BD AriaIII
Software	Analyzer:BD FACSDiva Data analysis: cytoflex cytexpert
Cell population abundance	all singlets were included

Gating strategy

FSC-H vs. FSC-A density plot gating was performed to identify singlets and SSC-A vs. FSC-A used to gate on intact cells and gate boundaries were defined based on untreated cells and then target cells quantified by fluorescence.

☒ Tick this box to confirm that a figure exemplifying the gating strategy is provided in the Supplementary Information.